 CMES, vol.1088, no.1, pp.1-35, 2009

Inverse Sensitivity Analysis of Singular Solutions of FRF matrix in Structural System Identification

S. Venkatesha[1], R. Rajender[2] and C. S. Manohar[3]

Abstract: The problem of structural damage detection based on measured frequency response functions of the structure in its damaged and undamaged states is considered. A novel procedure that is based on inverse sensitivity of the singular solutions of the system FRF matrix is proposed. The treatment of possibly ill-conditioned set of equations via regularization scheme and questions on spatial incompleteness of measurements are considered. The application of the method in dealing with systems with repeated natural frequencies and (or) packets of closely spaced modes is demonstrated. The relationship between the proposed method and the methods based on inverse sensitivity of eigensolutions and frequency response functions is noted. The numerical examples on a 5-degree of freedom system, a one span free-free beam and a spatially periodic multi-span beam demonstrate the efficacy of the proposed method and its superior performance *vis-a-vis* methods based on inverse eigensensitivity.

Keywords: Structural system identification; singular value decomposition; regularization; closely spaced modes; near periodic structures

1 Introduction

Structural characteristics, such as, spatial distribution of mass density, elastic properties, damping characteristics, boundary conditions and strength characteristics often undergo changes during the service life of a structure. These changes could be due to continued exposure of structures to hostile environments or due to episodic overloading conditions caused due to rare events such as strong motion earthquakes, passage of heavy vehicle on a bridge or cyclonic winds. These changes

[1] Technical Officer

[2] ME student; presently with General Eelctric India Technology Centre, Bangalore.

[3] Professor, Author for correspondence; email: manohar@civil.iisc.ernet.in; phone: 91 80 2293 3121; Fax: 91 80 2360 0404. Department of Civil Engineering, Indian Institute of Science, Bangalore 560 012 India

to the structural properties could be termed as "damage". From the point of view of monitoring the health of the structure, it is of vital importance to detect such changes to the structural properties either, as and when they occur, or, by deliberate inspection in the aftermath of overload conditions. One of the means to achieve this objective has been to analyze the vibration data emanating from the damaged structure with a view to detect, locate and quantify the structural damages.

Frequency response functions (FRF-s) constitute important descriptors of linear, time invariant dynamical systems. Among many of their attributes which render them important, especially in the context of structural system identification (SSI) and health monitoring (SHM), the main ones are as follows: (a) FRF-s are the primary quantities that are measured and the procedures for their measurement are widely studied and standardized (Ewins 2000, McConnel 1995), (b) they encapsulate information on system natural frequencies, mode shapes and damping characteristics and procedures for extracting this information from measured FRF-s are widely available (Maia and Silva 1997), (c) FRF-s are typically obtained by averaging across an ensemble of sample measurements and consequently, the effect of measurement noise is mitigated to a large extent (Bendat and Piersol 1982), (d) based on singular value decomposition of the FRF matrix, it is possible to delineate closely spaced and repeated natural frequencies (Shih *et al.* 1988, Allemang and Brown 1998), and (e) FRF-s permit computational prediction of structural performance to a wide range of loads that may be difficult to simulate in a laboratory condition (Meirovich 1984). These virtues make them particularly suited for SSI and structural damage detection (SDD) based on vibration data. The present study considers questions related to this area of research. Specifically, we consider the application of sensitivity of singular solutions of FRF-matrix in problems of SSI and SDD in systems with closely spaced modes. To highlight the relevance of this proposition, we briefly review the related literature. A detailed review of the relevant literature is available in the thesis by Venkatesha (2007).

The paper by Doebling *et al.,* (1998) provides a comprehensive review of methods to characterize structural damage based on vibration response and this review has been updated by Sohn *et al.,* (2003). Hseih *et al.,* (2006) examine experimental approaches based on ambient vibration, forced vibration and free vibration monitoring. Issues related to experimental methods for the purpose of condition assessment of existing structures have been discussed by Aktan *et al.,* (1997). Salawu (1997) has assessed the use of changes in natural frequencies to characterize structural damage. Peeters and Roeck (2001) review system identification methods based on vibration data emanating from operational loads, such as, those caused due to wind and vehicular traffic. The book by Friswell and Mottershead (1996) covers the principles of finite element model updating using vibration data with emphasis on

methods that use modal data and frequency domain data. The methods for SDD and SSI based on vibration data could be grouped into the following broad categories: direct matrix methods, methods based on real and complex valued eigensolutions, methods based on frequency response functions, method based on anti-resonance frequencies, and time domain methods (Venkatesha 2007). In the present study we focus on the methods based on eigensolutions and FRF-s. One of the early studies that employed changes in natural frequencies to characterize structural damage has been by Cawley and Adams (1979) and some of the recent studies on this line include the works of Hearn and Testa (1991), Farhat and Hemez (1993), Lin *et al.,* (1995), Lee and Jung (1997a,b), Law *et al.,* (1998), Sanayei *et al.,* (1999), Ge and Liu (2005), and Alvandi and Cremona (2005). The approach here typically consists of forming the matrix of first order eigen-derivatives with respect to system parameters of interest and using this matrix to relate the observed changes in modal characteristics to the structural damage using matrix pseudoinverse theory. Some of the complicating features that need to be addressed here include: the complex nature of modal characteristics due to presence of damping, possibility of repeated and (or) closely spaced modes, and simultaneous use of natural frequencies and mode shapes in parameter identification. As has already been noted, FRF-s are often the primary response characteristics which are measured first and eigen-characteristics are to be deduced from the measured FRF-s. The difficulties associated with modal extraction could be avoided if FRF-s are used directly in the problems of SSI and SDD. This approach has been investigated by Nobari (1991), Visser (1992), Wang *et al.,* (1997), Ratcliffe (2000), Lee and Kim (2001), Maia *et al.,* (2003), Cha and Switkes (2002), Park and Park (2003), and Huynh *et al.,* (2005). Forth and Staroselsky (2005) have developed a new hybrid surface-integral-finite-element numerical scheme to model a three-dimensional crack propagating through a thin, multi-layered coating and have discussed the mechanical issues of implementing a structural health monitoring system in an aircraft engine environment. In a recent paper Reddy and Ganguli (2007) have employed Fourier analysis of mode shapes and have introduced a damage index in terms of vector of Fourier coefficients. A related inverse problem of estimating applied time dependent forces on a beam using an iterative regularization scheme has been investigated by Huang and Shih (2007). Characterization of degradation in composite beams using a wave based approach that employs wavelet based spectral finite element scheme has been developed by Tabrez *et al.,* (2007). A demonstration on the application of natural neighbour Petrov-Galerkin (NNPG) method in design sensitivity analysis in 2D elasticity is made in the work reported by Kai Wang, *et al.,* (2008). In this investigation, the calculation of derivatives of shape functions with respect to design variables is avoided but instead the local weak form of governing equation is directly differentiated with respect to design variables and discretized with NNPG to obtain

the sensitivities of structural responds. An inverse vibration problem to simultaneously estimate the time-dependent damping and stiffness functions has been addressed by Chein-Shan Liu (2008) and it is shown that the proposed Lie-group shooting method can be employed to identify viscoelastic property of time-aging materials.

One of the problems associated with the use of FRF-s for SDD and SSI is that this method results in relatively larger number of equations (than those obtained, for instance, in the eigensensitivity method) governing the changes in system parameters which, subsequently, leads to numerical difficulties in finding the optimal solution. An alternative approach, which could possibly avoid this difficulty, would be to employ singular solutions and singular vectors associated with the measured FRF matrix in the SDD and SSI algorithms. The expectation here is that the singular solutions afford FRF data reduction and at the same time capture the essential features of the FRF-s in a succinct manner. In this context it is of interest to note that the spectra of singular values of measured FRF matrix have been used in the existing literature as markers of natural frequencies of the system (Shih *et al* 1988, Allemang and Brown 1998, Necati *et al.,* 2004). The question of utilizing the sensitivity of singular values and singular vectors in SSI and SDD seem to have been not addressed in the existing literature. Such an approach is expected to provide useful tools to study systems with closely spaced modes and repeated natural frequencies. As is well known, structures with repeated natural frequencies, typically arise in systems which display spatial symmetries. Similarly, systems with closely spaced modes are encountered in the study of large scale flexible structures (such as, piping in nuclear reactor structure). Moreover, for structures that possess spatial periodicity, such as turbine blades, stiffened shells, and multi-span beam and plate structures, the natural frequencies are known to occur in clusters of closely spaced modes with each of the clusters lying in pass bands of the system (Brillouin 1958, Sengupta 1980, Mead 1996). Any occurrence of a disorder in such systems results in localization of normal modes leading to spatial confinement of vibration energy (Hodges 1982, Manohar and Ibrahim 1999). We propose in this study to address the problem of SSI and SDD in systems with repeated modes and (or) closely spaced modes using changes in singular solutions of FRF matrix as the response feature for anomaly detection.

2 Singular solutions of FRF matrix and their derivatives

The equilibrium equations governing the dynamics of a N degrees-of-freedom (dof) linear time invariant system, in time and frequency domains, are respectively given

by

$$\begin{aligned} &M\ddot{x}+C\dot{x}+Kx=f(t);x(0)=x_0;\dot{x}(0)=\dot{x}_0 \\ &[D(\omega)]X(\omega)=F(\omega) \end{aligned} \tag{1}$$

Here M, K, and C are respectively the $N \times N$ mass, stiffness and damping matrices; $D(\omega) = [-\omega^2 M + i\omega C + K]$ is the $N \times N$ complex valued dynamic stiffness matrix, $x(t) = N \times 1$ displacement vector, $f(t) = N \times 1$ force vector, $X(\omega)$= Fourier transform of $x(t)$, $F(\omega)$= Fourier transform of $f(t)$, t = time, ω = frequency, i = imaginary number and a dot over head represents derivative with respect to time t. Taking into account the assembling procedure followed in finite element formulation (Petyt 1998), the structural matrices can be represented in the form

$$K = \sum_{s=1}^{N_e} [A]_s^t [K]_s^e [A]_s \quad C = \sum_{s=1}^{N_e} [A]_s^t [C]_s^e [A]_s \tag{2}$$

Here the superscript e denotes the element, N_e is the number of finite elements and $[A]_s$ is the nodal connectivity matrix of size $NDOF \times N$ where $NDOF$ is the number of dofs in the s^{th} element. We assume that the measured FRF matrix is a $N_r \times N_s$ ($N_r \geq N_s, N_r, N_s \leq N$) matrix and this could denote the system receptance, mobility or accelerance. However, for the purpose of illustration, we assume that the measured FRF matrix corresponds to the $N_r \times N_s$ receptance matrix $\alpha(\omega)$. We introduce two matrices B and Q as

$$B(\omega) = \alpha(\omega)\alpha^T(\omega) \quad Q(\omega) = \alpha^T(\omega)\alpha(\omega) \tag{3}$$

Here, the superscript T represents the conjugate transpose. Clearly, B and Q are respectively of sizes $N_r \times N_r$ and $N_s \times N_s$. Furthermore, these matrices are real valued, symmetric in nature and the two matrices possess identical nonzero eigenvalues. Denoting by $U(\omega)$ and $V(\omega)$ the $N_r \times N_r$ and $N_s \times N_s$ eigenvector matrices of B and Q respectively, the matrix $\alpha(\omega)$ can be decomposed as

$$\alpha(\omega) = U(\omega)\Sigma(\omega)V^T(\omega) \tag{4}$$

Here $\Sigma(\omega)$ is a $N_r \times N_s$ matrix that has the following structure

$$\Sigma(\omega) = \begin{bmatrix} [\Lambda]_{N_s \times N_s} \\ [0]_{(N_r - N_s) \times N_s} \end{bmatrix}_{N_r \times N_s} \tag{5}$$

where Λ is the diagonal matrix that carries the non-zero eigenvalues of matrices B and Q. Equation 4 together with 5 constitute the singular value decomposition of

the FRF matrix $\alpha(\omega)$. The notion of a complex mode indicator function (CMIF) was introduced by Shih *et al.,* (1988) as

$$CMIF(\omega)_{N_s \times N_s} = [\Sigma(\omega)]^T_{N_s \times N_r} [\Sigma(\omega)]_{N_r \times N_s} \tag{6}$$

This function serves as a means for identification of model order and also for locating the natural frequencies. In using this indicator, the CMIF-s are plotted as a function of frequency ω with natural frequencies indicated by large values of the first CMIF and double or multiple modes by simultaneously large values of two or more CMIF values (Ewins 2000). The singular vectors, that is, the columns of matrices, $U(\omega)$ and $V(\omega)$, admit physical interpretation as follows: the left singular vector $U_1(\omega_r)$ evaluated at the r-th natural frequency ω_r, approximates the r-th mode shape; and, the right singular vector $V_1(\omega_r)$ represents the approximate force pattern necessary to generate a response only in the r-th mode. Here it is assumed that ω_r does not repeat. If this assumption is not valid, there will be as many left vectors and right vectors which correspond to the number of repeated modes. Appendix A provides a numerical example on a seven dof system in which one of the natural frequencies repeats six times and demonstrates the use of singular solutions of FRF matrix in detecting the repetition of the natural frequencies.

As has been already noted, we propose in this study to employ the singular solutions of measured FRF-s to develop algorithms for SSI and SDD. To achieve this, we first need to obtain the derivatives of the singular solutions with respect to the system parameters of interest. We consider the eigenvalue problem $Qy = \lambda y$ and, corresponding to the i-th eigenpair (λ_i, y_i), we obtain the equation $F_i y_i = 0$ with $F_i = Q - \lambda_i I$ where I is the identity matrix. Let $\{p_i\}_{i=1}^n$ denote the system parameters of interest. From the equation $F_i y_i = 0$ it follows that $y_i^T(p) F_i(p) y_i(p) = 0$. Differentiating this function with respect to p_j we get

$$\frac{\partial y_i^T}{\partial p_j} F_i y_i + y_i^T \frac{\partial F_i}{\partial p_j} y_i + y_i^T F_i \frac{\partial y_i}{\partial p_j} = 0 \tag{7}$$

By noting that $F_i y_i = 0$, it follows that $y_i^T F_i^T = y_i^T F_i = 0$, leading to

$$y_i^T \frac{\partial F_i}{\partial p_j} y_i = 0 \tag{8}$$

Similarly, by noting that $F_i = Q - \lambda_i I$, we get

$$y_i^T \left[\frac{\partial Q}{\partial p_j} - \frac{\partial \lambda_i}{\partial p_j} I \right] y_i = 0 \tag{9}$$

Simplifying this expression we further obtain

$$\frac{\partial \lambda_i}{\partial p_j} = y_i^T \left[\frac{\partial Q}{\partial p_j} \right] y_i \tag{10}$$

To obtain derivative of the eigenvectors with respect to p we consider two modes y_i and y_s and note that

$$y_i^T y_s = \delta_{is}$$

$$y_i^T Q y_s = \lambda_i \delta_{is} \tag{11}$$

where δ_{is} is the Kronecker delta function. Differentiating equation (11 a), with respect to p_j, we get

$$\frac{\partial y_i^T}{\partial p_j} y_s + y_i^T \frac{\partial y_s}{\partial p_j} = 0. \tag{12}$$

Since $\frac{\partial y_i^T}{\partial p_j} y_s$ and $y_i^T \frac{\partial y_s}{\partial p_j}$ are scalars, we can write

$$y_s^T \frac{\partial y_i}{\partial p_j} + y_i^T \frac{\partial y_s}{\partial p_j} = 0. \tag{13}$$

Similarly, by differentiating equation (11 b), with respect to p_j we get

$$y_s^T Q \frac{\partial y_i}{\partial p_j} + y_i^T Q \frac{\partial y_s}{\partial p_j} = \frac{\partial \lambda_i}{\partial p_j} \delta_{is} - y_i^T \frac{\partial Q}{\partial p_j} y_s. \tag{14}$$

Furthermore, by using the conditions$F_i y_i = 0$, we get additional equations

$$\begin{aligned} F_i \frac{\partial y_i}{\partial p_j} &= -\frac{\partial F_i}{\partial p_j} y_i \\ F_s \frac{\partial y_s}{\partial p_j} &= -\frac{\partial F_s}{\partial p_j} y_s \end{aligned} \tag{15}$$

Thus, equations (13-15) can be combined to get

$$\begin{bmatrix} F_i & 0 \\ 0 & F_s \\ y_s^T & y_i^T \\ y_s^T Q & y_i^T Q \end{bmatrix} \begin{Bmatrix} \frac{\partial y_i}{\partial \delta_j} \\ \frac{\partial y_s}{\partial \delta_j} \end{Bmatrix} = \begin{bmatrix} -\frac{\partial F_i}{\partial \delta} y_i \\ -\frac{\partial F_s}{\partial \delta} y_s \\ 0 \\ \frac{\partial \lambda_i}{\partial \delta_j} \delta_{is} - y_i^T \frac{\partial Q}{\partial \delta_j} y_s \end{bmatrix} \tag{16}$$

In deriving the above equation we have considered only the eigenpairs (λ_i, y_i) and (λ_s, y_s). We could develop equations similar to equation (16) by considering more than two eigenpairs. Thus, for the case of 3 eigenpairs (λ_i, y_i), (λ_r, y_r) and (λ_s, y_s), the following equation for eigenvector sensitivity can be derived.

$$\begin{bmatrix} F_i & 0 & 0 \\ 0 & F_r & 0 \\ 0 & 0 & F_s \\ y_r^T & y_i^T & 0 \\ y_r^T Q & y_i^T Q & 0 \\ y_s^T & 0 & y_i^T \\ y_s^T Q & 0 & y_i^T Q \\ 0 & y_s^T & y_r^T \\ 0 & y_s^T Q & y_r^T Q \end{bmatrix} \begin{Bmatrix} \frac{\partial y_i}{\partial p_j} \\ \frac{\partial y_r}{\partial p_j} \\ \frac{\partial y_s}{\partial p_j} \end{Bmatrix} = \begin{bmatrix} -\frac{\partial F_i}{\partial p_j} y_i \\ -\frac{\partial F_r}{\partial p_j} y_r \\ -\frac{\partial F_s}{\partial p_j} y_s \\ 0 \\ \frac{\partial \lambda_i}{\partial \delta_j}\delta_{ir} - y_i^T \frac{\partial Q}{\partial \delta_j} y_r \\ 0 \\ \frac{\partial \lambda_i}{\partial \delta_j}\delta_{is} - y_i^T \frac{\partial Q}{\partial \delta_j} y_s \\ 0 \\ \frac{\partial \lambda_i}{\partial \delta_j}\delta_{rs} - y_r^T \frac{\partial Q}{\partial \delta_j} y_s \end{bmatrix} \tag{17}$$

Similarly, for four eigenpairs with indices i, r, s, k one gets,

$$\begin{bmatrix} F_i & 0 & 0 & 0 \\ 0 & F_r & 0 & 0 \\ 0 & 0 & F_s & 0 \\ 0 & 0 & 0 & F_k \\ y_r^T & y_i^T & 0 & 0 \\ y_r^T Q & y_i^T Q & 0 & 0 \\ y_s^T & 0 & y_i^T & 0 \\ y_s^T Q & 0 & y_i^T Q & 0 \\ y_k^T & 0 & 0 & y_i^T \\ y_k^T Q & 0 & 0 & y_i^T Q \\ 0 & y_s^T & y_r^T & 0 \\ 0 & y_s^T Q & y_r^T Q & 0 \\ 0 & y_k^T & 0 & y_r^T \\ 0 & y_k^T Q & 0 & y_r^T Q \\ 0 & 0 & y_k^T & y_s^T \\ 0 & 0 & y_k^T Q & y_s^T Q \end{bmatrix} \begin{Bmatrix} \frac{\partial y_i}{\partial p_j} \\ \frac{\partial y_r}{\partial p_j} \\ \frac{\partial y_s}{\partial p_j} \\ \frac{\partial y_k}{\partial p_j} \end{Bmatrix} = \begin{bmatrix} -\frac{\partial F_i}{\partial p_j} y_i \\ -\frac{\partial F_r}{\partial p_j} y_r \\ -\frac{\partial F_s}{\partial p_j} y_s \\ -\frac{\partial F_k}{\partial p_j} y_k \\ 0 \\ \frac{\partial \lambda_i}{\partial \delta_j}\delta_{ir} - y_i^T \frac{\partial Q}{\partial \delta_j} y_r \\ 0 \\ \frac{\partial \lambda_i}{\partial \delta_j}\delta_{is} - y_i^T \frac{\partial Q}{\partial \delta_j} y_s \\ 0 \\ \frac{\partial \lambda_i}{\partial \delta_j}\delta_{ik} - y_i^T \frac{\partial Q}{\partial \delta_j} y_k \\ 0 \\ \frac{\partial \lambda_i}{\partial \delta_j}\delta_{rs} - y_r^T \frac{\partial Q}{\partial \delta_j} y_s \\ 0 \\ \frac{\partial \lambda_i}{\partial \delta_j}\delta_{rk} - y_r^T \frac{\partial Q}{\partial \delta_j} y_k \\ 0 \\ \frac{\partial \lambda_i}{\partial \delta_j}\delta_{sk} - y_s^T \frac{\partial Q}{\partial \delta_j} y_k \end{bmatrix} \tag{18}$$

The sensitivity of eigensolutions of the matrix B can also be derived on similar lines.

3 Inverse sensitivity analysis

The derivatives of singular solutions developed in the preceding section are now used in developing a SDD algorithm. Let $\Gamma_k(p_1, p_2, \cdots, p_n)$, $k = 1, 2, \cdots, N_k$, denote a generic set of dynamic characteristics of the system. This set includes a selection of singular values and elements of singular vectors at a chosen set of driving frequency points. It is assumed that $\Gamma_k(p_1, p_2, \cdots, p_n)$, $k = 1, 2, \cdots, N_k$ are differentiable with respect to $\{p_i\}_{i=1}^n$ to a desired level. Furthermore, let $p_u = \{p_{ui}\}_{i=1}^n$ represent the system characteristics in its undamaged state. We write $p_{di} = p_{ui} + \Delta_i$ where Δ_i is the change in the i^{th} system parameter due to the occurrence of damage. Based on these notations and using Taylor's expansion, we can write,

$$\Gamma_k[p_{u1}+\Delta_1, p_{u2}+\Delta_2, \cdots, p_{un}+\Delta_n] = \Gamma_k[p_{u1}, p_{u2}, \cdots, p_{un}] + \sum_{i=1}^{n} \left.\frac{\partial \Gamma_k}{\partial p_{ui}}\right|_{p=p_u} \Delta_i + \frac{1}{2}\sum_{i=1}^{n}\sum_{j=1}^{n} \left.\frac{\partial^2 \Gamma_k}{\partial p_{ui}\partial p_{uj}}\right|_{p=p_u} \Delta_i\Delta_j + \cdots \tag{19}$$

The quantity $\Delta\Gamma_k = \Gamma_k\{p_{d1}, p_{d2}, \cdots, p_{dn}\} - \Gamma_k\{p_{u1}, p_{u2}, \cdots, p_{un}\}$ represents the change in the character Γ_k due to occurrence of damage and this quantity is expected to be measured based on experiments conducted on the structure in its damaged and undamaged states. The essence of first order damage detection methods consist of writing equation (19) as

$$\Delta\Gamma_k = \sum_{i=1}^{n} \left.\frac{\partial \Gamma_k}{\partial p_{ui}}\right|_{p=p_u} \Delta_i; \quad k = 1, 2, \cdots, N_k \tag{20}$$

This can be re-written as

$$\{\Delta\Gamma\}_{N_k\times 1} = [S]_{N_k\times n}\{\Delta\}_{n\times 1} \tag{21}$$

It is emphasized that the matrix $[S]$ is evaluated for the structure in its undamaged state. Consequently, the damage vector $\{\Delta\}$ is obtained as

$$\{\Delta\} = [S]^{+}\{\Delta\Gamma\} \tag{22}$$

where + denotes the matrix pseudo-inverse. It may be noted that this determination of Δ crucially depends upon the matrix $[S]$ being well conditioned. Often, this requirement may not be met in applications due to, for example, presence of measurement noise, and it would become necessary to employ regularization

techniques to obtain acceptable solutions. To apply the scheme, equation 22 is re-written as $[S^t S + \xi I]\{\Delta\} = S^t \Delta\Gamma$. Here ξ is called the regularization parameter and it is selected such that the matrix $[S^t S + \xi I]$ is not ill-conditioned. Thus, Δ is now determined using $\{\Delta\} = [S^t S + \xi I]^{-1} S^t \Delta\Gamma$. This solution can be shown as being equivalent to finding Δ such that $||S\Delta - \Delta\Gamma|| + \xi||\Delta||$ is minimized (Hansen 1994). The first term here represents the error norm and the second term the smoothness of the solution. It is clear that ξ cannot be made arbitrarily large, in which case, the physical characteristic of the original problem would be distorted; on the other hand, if ξ=0, the solution to the problem is not satisfactory, if not impossible. Thus in the selection of ξ, a trade-off is involved, and, in implementing the regularization scheme a 'L'-curve that represents $||S\Delta - \Delta\Gamma||$versus $||\Delta||$is constructed for different values of ξ. The value of ξthat corresponds to the knee of this curve is taken as being optimal. It may also be noted that in equation 20, the Taylor expansion has been carried out around $\{p_u\}$, the system parameters in the undamaged state, and the S matrix in equation 21 is evaluated at this initial guess. The reference value around which the Taylor expansion is done can be updated once an estimate of Δ is obtained using equation 22. This leads to an iterative strategy to solve for Δ as follows: $\{\Delta\}_{\bar{k}+1} = [S]_{\bar{k}} + \{\Delta\Gamma\}_{\bar{k}}$; $\bar{k} = 1, 2, \cdots, N_T$. This iteration could be stopped based on a suitable convergence criterion based on difference in norms of initial guess and predicted value of Δ.

4 Illustrative examples

The SDD method outlined in the preceding section is now illustrated using a 5-dof discrete system, a one span free-free beam and a spatially periodic four span continuous beam. The example on free-free beam includes data from experimental studies. The range of issues covered include effect of damage on systems with repeated natural frequencies, effect of spatial incompleteness of measurements, damages in periodic structures in which natural frequencies occur in clusters and occurrence of damage herein could lead to normal mode localization. In all the numerical examples considered, the governing equations for the damage indicator factors have been solved by incorporating regularization scheme.

4.1 A five degrees-of freedom system

In this example, we consider the 5-dof system shown in figure 1. By adjusting the parameters of this model we create following three scenarios:

a. the structure in its undamaged state has one of its natural frequencies repeating twice and the damaged structure possess five distinct natural frequencies,

b. the structure in its damaged as well as undamaged states has two of its natural frequencies repeating twice, and

c. the structure in its undamaged state has five distinct natural frequencies while the damaged structure has one of its natural frequencies repeating twice.

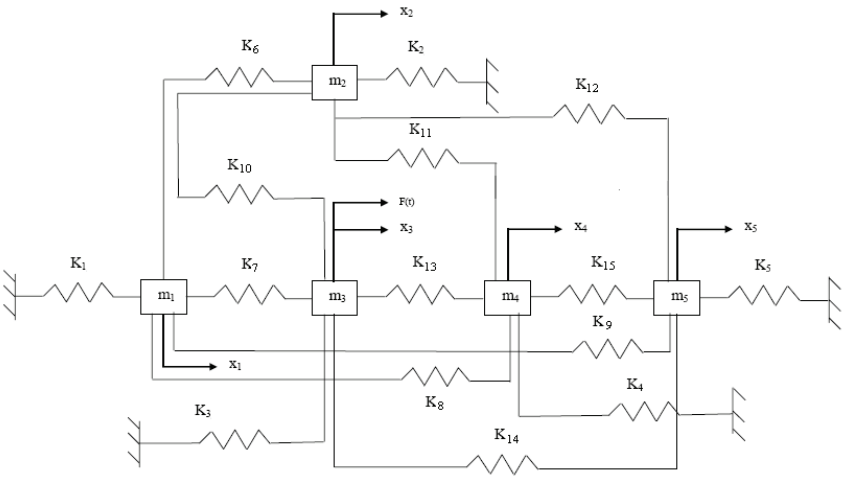

Figure 1: Five-dof system considered in section 5.1.

The SDD algorithm used in this section to tackle these problems employs only the information on sensitivity of singular values. The system parameters in damaged state are taken to be related to the corresponding parameters in undamaged state through the relation $m_{di} = \alpha_i m_{ui}$; $i = 1, 2, \cdots 5$ and $k_{di} = \beta_i k_{ui}$; $i = 1, 2, \cdots 15$. For the purpose of illustration it is assumed that damping is classical with the damping parameter for all modes being constant. The occurrence of the damage is taken not to affect the damping. In each of the examples, a frequency range of 0-30 rad/s with $\Delta\omega$=0.1 rad/s is considered. The spectra of singular values are extracted from the 5×5 receptance matrix and all the five singular values are used in SDD. To facilitate the comparison of the performance of the proposed method (Method I) we also analyze the problem using inverse sensitivity of system natural frequencies and mode shapes (Method II) the details of which are available in existing literature (see, for example, the thesis by Venkatesha 2007).

Case (a): Table 1 summarizes the system parameters in its undamaged state. Here $\omega_3 = \omega_4$=16.33 rad/s –a fact that could also be ascertained from the spectra of singular values shown in figure 2. The system is taken to have a modal damping of

5% in all the modes. The structure in its damaged state is considered with

$\alpha_1 = 0.91, \quad \alpha_2 = 0.91, \quad \alpha_3 = 0.91, \quad \alpha_4 = 0.91, \quad \alpha_5 = 0.91, \quad \beta_1 = 0.95,$
$\beta_2 = 0.96, \quad \beta_3 = 0.95, \quad \beta_4 = 0.95, \quad \beta_5 = 0.94, \quad \beta_6 = 0.95, \quad \beta_7 = 0.95,$
$\beta_8 = 0.95, \quad \beta_9 = 0.95, \quad \beta_{10} = 0.95, \quad \beta_{11} = 0.95, \quad \beta_{12} = 0.95, \quad \beta_{13} = 0.95,$
$\beta_{14} = 0.95, \quad \text{and} \quad \beta_{15} = 0.95.$

The undamped system natural frequencies and mode shapes now get modified as

$$\omega_n = \begin{pmatrix} 10.2250 & 15.6729 & 16.6850 & 16.7070 & 23.5337 \end{pmatrix} \text{ rad/s}$$

$$\Phi = \begin{bmatrix} 0.0280 & -0.0192 & 0.0428 & 0.0245 & -0.0087 \\ 0.0279 & -0.0186 & -0.0000 & -0.0496 & -0.0088 \\ 0.0280 & -0.0192 & -0.0428 & 0.0245 & -0.0087 \\ 0.0281 & 0.0439 & -0.0000 & 0.0003 & -0.0056 \\ 0.0281 & -0.0050 & -0.0000 & -0.0002 & 0.1009 \end{bmatrix}.$$

It may be noted that in the damaged system all the natural frequencies are distinct. The results of damage detection using inverse sensitivity on singular values (Method I) are shown in figures 3 and 4. It may be observed that the SDD algorithm leads to satisfactory estimate of damaged system parameters. The solution to same problem by using inverse sensitivity of natural frequencies and mode shapes was also attempted. The algorithm in this case however, did not function satisfactorily: figure 5 shows a selection of these results which show unacceptable fluctuations in vales of mass parameters as iterations proceeds. This example provides an instance where the proposed SDD algorithm in this paper performs better than inverse eigensensitivity method that is available in the existing literature.

Case (b): The undamaged system as in Table 1 and the damaged system is simulated with

$\alpha_1 = 0.92, \quad \alpha_2 = 0.92, \quad \alpha_3 = 0.92, \quad \alpha_4 = 0.92, \quad \alpha_5 = 0.92, \quad \beta_1 = 0.9,$
$\beta_2 = 0.9, \quad \beta_3 = 0.9, \quad \beta_4 = 0.9, \quad \beta_5 = 0.9, \quad \beta_6 = 0.9, \quad \beta_7 = 0.9,$
$\beta_8 = 0.9, \quad \beta_9 = 0.9, \quad \beta_{10} = 0.9, \quad \beta_{11} = 0.9, \quad \beta_{12} = 0.9, \quad \beta_{13} = 0.9,$
$\beta_{14} = 0.9, \quad \text{and} \quad \beta_{15} = 0.9.$

The undamped eigensolutions for the damaged structure are as follows:

$$\omega_n = \begin{pmatrix} 9.8907 & 15.1685 & 16.1515 & 16.1515 & 22.8017 \end{pmatrix} \text{ rad/s}$$

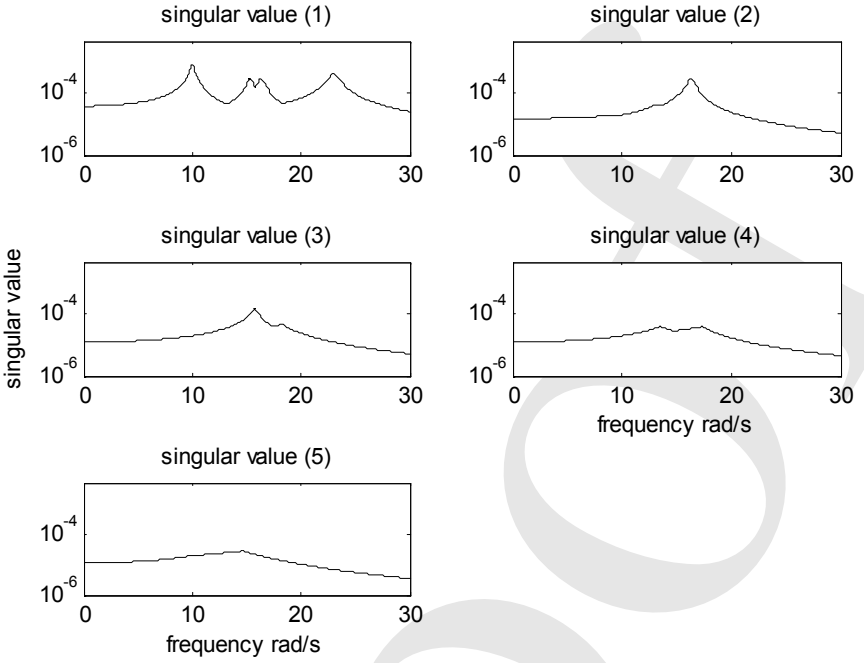

Figure 2: Example 5.1, Case (a); spectra of singular values of the structure in undamaged state

Table 1: Model parameters for the system considered in section 5.1 (figure 1).

Mass parameters M (kg)	$m = 100$, $m_1 = m_2 = m_3 = 3m$, $m_4 = 4m$, $m_5 = m$
Stiffness parameters K (N/m)	$k = 10000$, $k_1 = k_2 = 3k$, $k_3 = k$, $k_4 = 4k$, $k_5 = k$, $k_6 = k_7 = k_8 = k_9 = k_{10} = k_{11} = k_{12} = k_{13} = k_{14} = k_{15} = k$
Damping parameters $C_d = [2\eta_n\omega_n]$ (Ns/m)	C_{d1}= 2.0000, C_{d2}= 3.0672, C_{d3}=3.2660, C_{d4}= 3.2660, C_{d5}= 4.6107
Undamped natural frequency ω_n (rad/s)	ω_1=10.0000, ω_2=15.3361, ω_3=16.3299, ω_4=16.3299, ω_5=23.0536
Mass normalized undamped modal matrix Φ	$\begin{bmatrix} 0.0267 & -0.0181 & 0.0408 & -0.0236 & -0.0083 \\ 0.0267 & -0.0181 & -0.0408 & -0.0236 & -0.0083 \\ 0.0267 & -0.0181 & -0.0000 & 0.0471 & -0.0083 \\ 0.0267 & 0.0419 & 0.0000 & -0.0000 & -0.0054 \\ 0.0267 & -0.0047 & -0.0000 & 0.0000 & 0.0962 \end{bmatrix}$

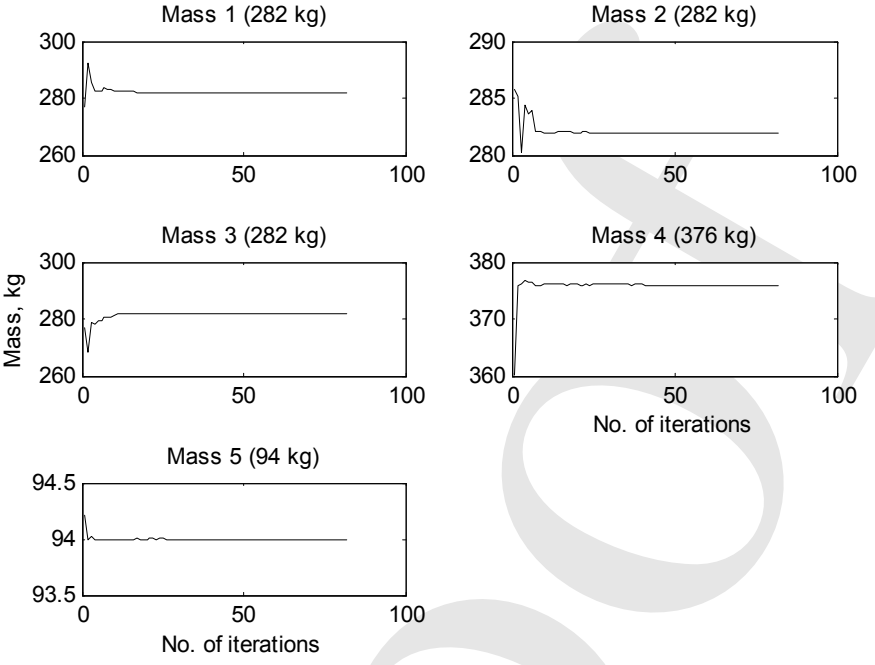

Figure 3: Example 5.1, Case (a); results from Method I; detection of changes to mass parameters; reference values of the parameters are shown in parenthesis.

$$\Phi = \begin{bmatrix} 0.0279 & -0.0189 & 0.0032 & 0.0490 & -0.0087 \\ 0.0279 & -0.0189 & -0.0441 & -0.0218 & -0.0087 \\ 0.0279 & -0.0189 & 0.0409 & -0.0273 & -0.0087 \\ 0.0279 & 0.0437 & 0.0000 & 0.0000 & -0.0056 \\ 0.0279 & -0.0049 & -0.0000 & 0.0000 & 0.1003 \end{bmatrix}.$$

Here it may be noted that both the damaged and undamaged structures have one of their natural frequencies repeating twice. Here again it was observed that Method I performed better than Method II. Figure 6 shows the SDD iterations on the mass parameter using Method I. Interestingly, results from Method II showed convergent behavior (Figure 7) but the values to which the SDD algorithm converged to were unsatisfactory.

Case (c): The undamaged system is now taken have the properties

$m_1 = 282, m_2 = 282, m_3 = 282, m_4 = 376, m_5 = 94$ (kg) and

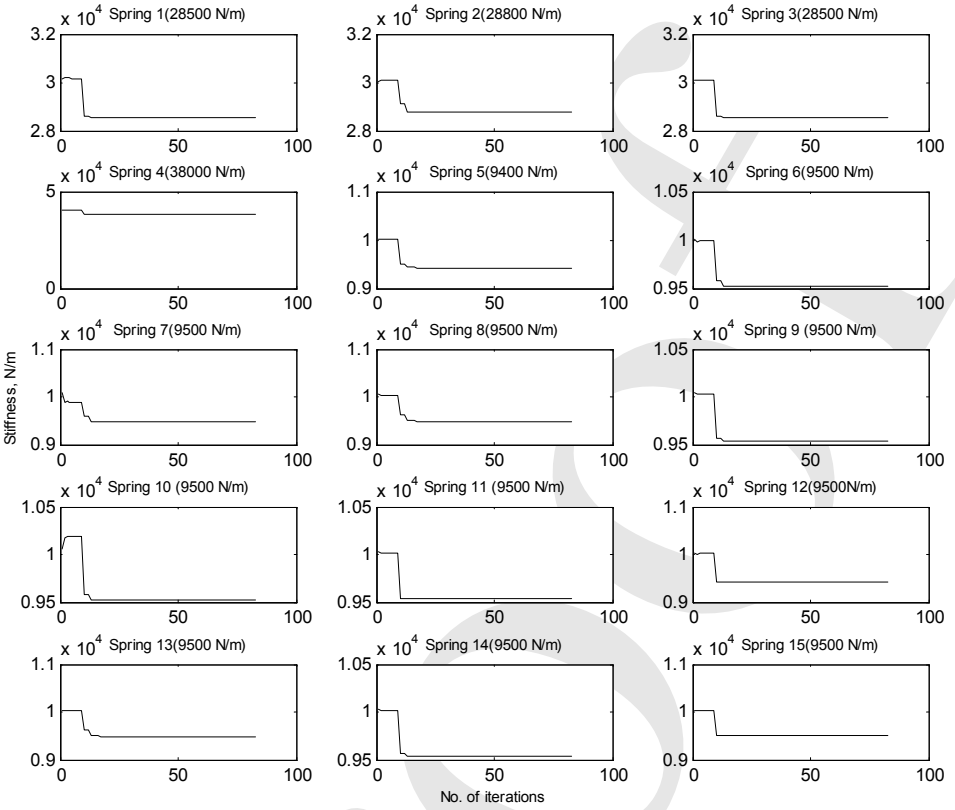

Figure 4: Example 5.1, Case (a); results from Method I; detection of changes to stiffness parameters; reference values of the parameters are shown in parenthesis.

$$k_{1g} = 28500, \quad k_{2g} = 28800, \quad k_{3g} = 28500, \quad k_{4g} = 38000, \quad k_{5g} = 9400,$$
$$k_{12} = 9500, \quad k_{13} = 9500, \quad k_{14} = 9500, \quad k_{15} = 9500, \quad k_{23} = 9500,$$
$$k_{24} = 9500, \quad k_{25} = 9500, \quad k_{34} = 9500, \quad k_{35} = 9500, \quad k_{45} = 9500 \text{ (N/m)}$$

The natural frequencies and mode shapes of this system are obtained as

$$\omega_n = \begin{pmatrix} 10.0605 & 15.4207 & 16.4166 & 16.4382 & 23.1551 \end{pmatrix} \text{ rad/s}$$

$$\Phi = \begin{bmatrix} 0.0276 & -0.0189 & 0.0421 & 0.0241 & -0.0086 \\ 0.0274 & -0.0183 & -0.0000 & -0.0488 & -0.0086 \\ 0.0276 & -0.0189 & -0.0421 & 0.0241 & -0.0086 \\ 0.0276 & 0.0432 & 0.0000 & 0.0003 & -0.0056 \\ 0.0276 & -0.0049 & -0.0000 & -0.0002 & 0.0992 \end{bmatrix}.$$

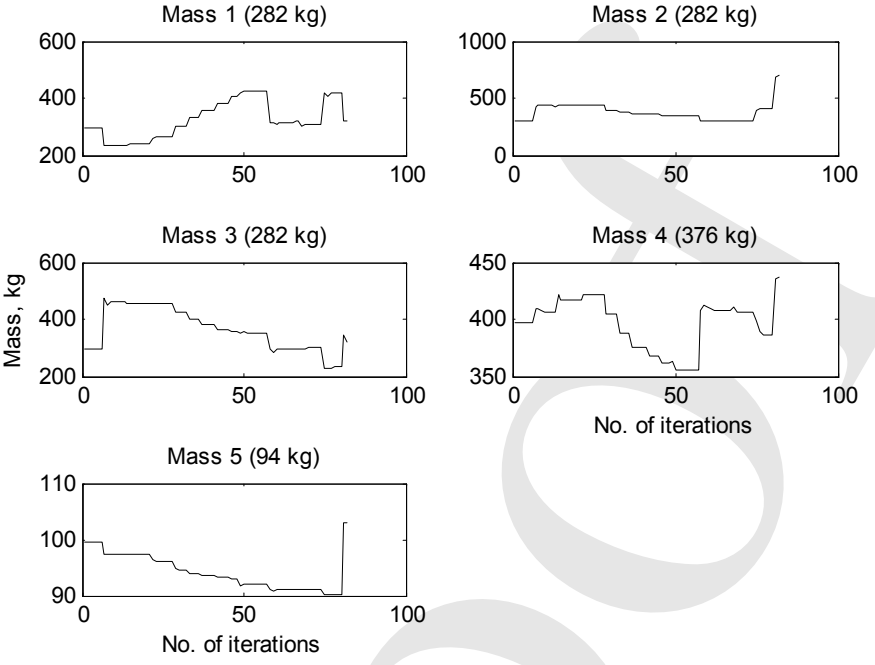

Figure 5: Example 5.1, Case (a); results from Method II; detection of changes to mass parameters; reference values of the parameters are shown in parenthesis.

Now we form the damaged system with

$m_1 = 300, \quad m_2 = 300, \quad m_3 = 300, \quad m_4 = 400, \quad m_5 = 100$ (kg) and

$$k_{1g} = 30000, \quad k_{2g} = 30000, \quad k_{3g} = 30000, \quad k_{4g} = 40000, \quad k_{5g} = 10000,$$
$$k_{12} = 10000, \quad k_{13} = 10000, \quad k_{14} = 10000, \quad k_{15} = 10000, \quad k_{23} = 10000,$$
$$k_{24} = 10000, \quad k_{25} = 10000, \quad k_{34} = 10000, \quad k_{35} = 10000, \quad k_{45} = 10000 \text{ (N/m)}$$

The undamped eigensolutions for this system are obtained as

$$\omega_n = \begin{pmatrix} 10.0000 & 15.3361 & 16.3299 & 16.3299 & 23.0536 \end{pmatrix} \text{ rad/s}$$

$$\Phi = \begin{bmatrix} 0.0267 & -0.0181 & 0.0408 & -0.0236 & -0.0083 \\ 0.0267 & -0.0181 & -0.0408 & -0.0236 & -0.0083 \\ 0.0267 & -0.0181 & -0.0000 & 0.0471 & -0.0083 \\ 0.0267 & 0.0419 & 0.0000 & -0.0000 & -0.0054 \\ 0.0267 & -0.0047 & -0.0000 & 0.0000 & 0.0962 \end{bmatrix}.$$

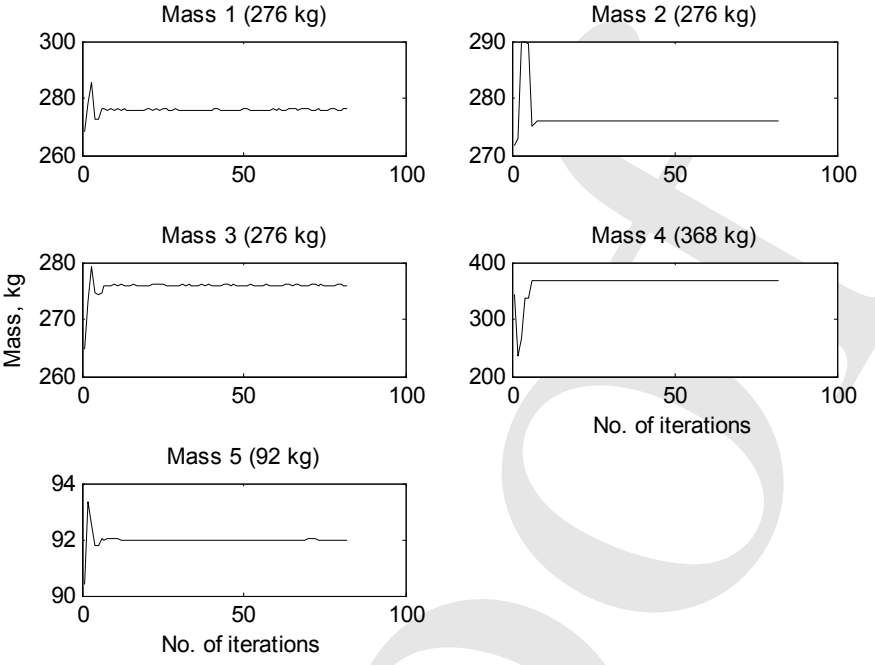

Figure 6: Example 5.1, Case (b); results from Method I; detection of changes to mass parameters; reference values of the parameters are shown in parenthesis.

Here it is may be noted that the structure in its undamaged state has five distinct natural frequencies while the damaged structure has one of its natural frequency repeating twice. Here again, it was observed that while Method I performed satisfactorily (Figure 8), Method II, on the other hand showed unsatisfactory convergence behavior (Figure 9).

4.2 A one span free-free beam

A 0.78 m span free-free steel beam as shown in figure 10 is considered in this example (figure 10). The beam, in its undamaged state, carries a concentrated mass M=0.027 kg as shown and the damaged structure is simulated by removing this mass from the structure. The system FRF-s in this case were simulated synthetically with (with E=2.0$\times 10^{11}$ N/m^2, ρ=7528.9 kg/m^3) and also measured experimentally in a laboratory using impulse hammer technique. The structure was modeled using 50 numbers of 2-noded Euler-Bernoulli beam elements with 2-dof per node. For the purpose of damage detection, the beam was divided into five equal zones with similar elastic and mass properties. The removal of mass, as mentioned

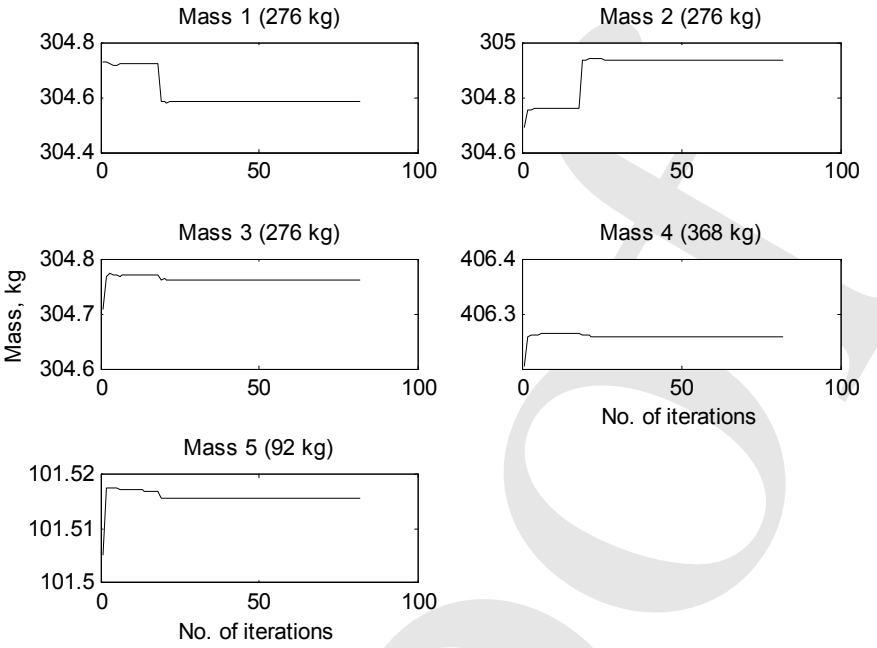

Figure 7: Example 5.1, Case (b); results from Method II; detection of changes to mass parameters; the SDD algorithm does not converge to the reference values shown in parenthesis.

above, results in zone 3 suffering a 6.65% loss of mass. Consequently, the reference value of the damage indicator factor α_3 is 0.9335 and, since no other elements suffer either loss of mass and/or loss of stiffness, the reference damage indicating factors for the remaining zones remain as 1.000 for both mass and stiffness parameters. The size of the FRF matrix used in damage detection in this case was taken to be 6×1thereby introducing the issue of spatial incompleteness of measurements into the SDD procedure. In this example, both Methods I and II (as per the nomenclature of the preceding section) show satisfactory performance. Method I is implemented using the spectra of one singular value and one left singular vector. Method II is implemented using sensitivity of first three natural frequencies and mode shapes. Figure 11 shows a selection of results obtained using Method II based on synthetic data. The Nyquist plot of one of the FRF of the system before and after the damage detection using Methods I and II are shown in figure 12. It may be noted that the damage detection using both Methods I and II are equally successful and consequently the difference in the predicted FRF-s from the two methods cannot be delineated in this figure. Damage detection using experimen-

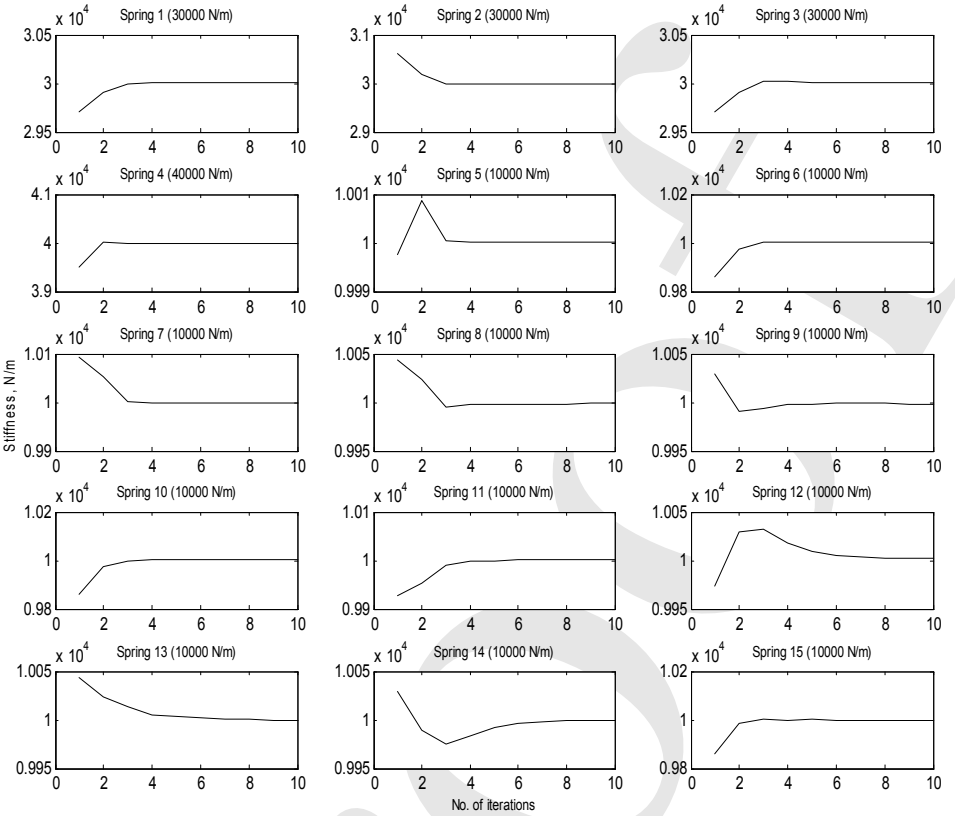

Figure 8: Example 5.1, Case (c); results from Method I; detection of changes to stiffness parameters; the reference values of the parameters are shown in the parenthesis.

tally measured FRF-s with Method II was possible with about 5% accuracy and figure 13 shows a comparison of FRF measured on the damaged system with the corresponding prediction using estimated parameters after damage detection.

4.3 A four span spatially periodic continuous beam

The example structure here is representative of spatially periodic structures and this class of structures are known to display several unusual dynamic characteristics (Brillouin 1958, Sengupta 1980, Mead 1996). The dynamic response of these structures is characterized by alternating sequence of frequency bands which pass or stop traveling waves. The system natural frequencies here occur in clusters within the pass bands with the number of natural frequencies within each clus-

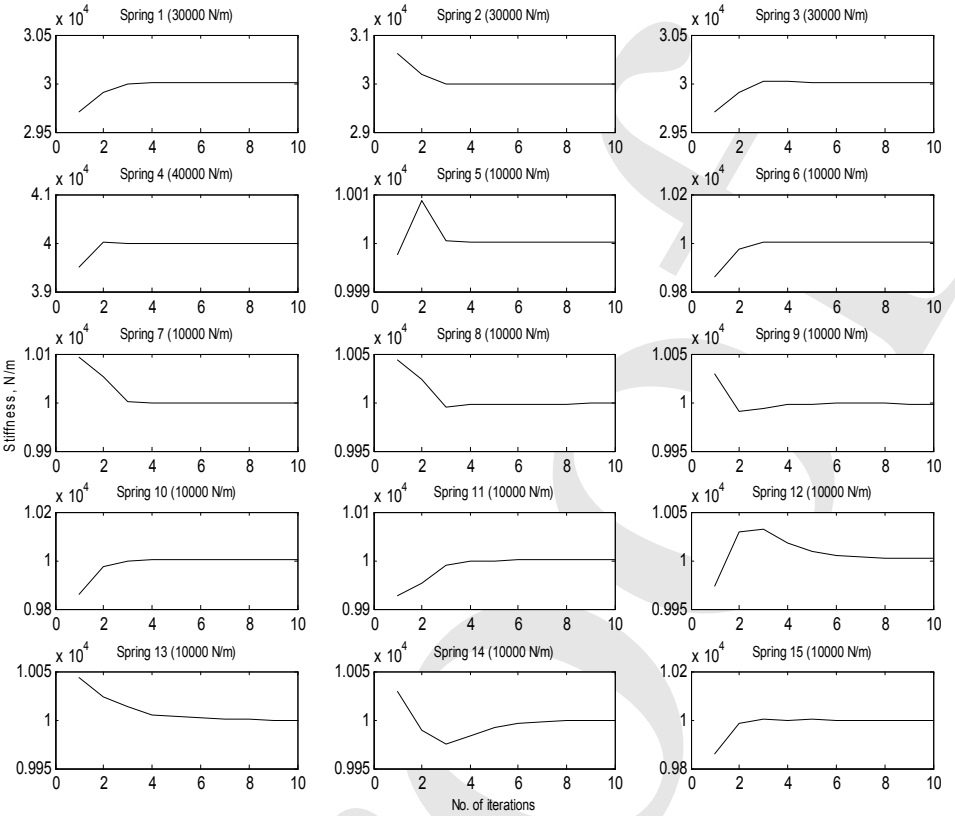

Figure 9: Example 5.1, Case (c); results from Method II; detection of changes to stiffness parameters; the SDD algorithm does not converge to the reference values shown in parenthesis.

ter being equal to the number of repetitive units in the structure. If any of the structural properties are modified so as break the spatial periodicity, the resulting disordered system displays the phenomena of normal mode localization (Hodges 1982, Manohar and Ibrahim 1999). Thus, this class of structures offers interesting challenges in SSI and SDD. To clarify some of these features, we begin by considering a harmonically driven one span beam unit as shown in figure 14. Using transfer matrix formalism, the steady state amplitude of the harmonic bending moment and rotation at the right end can be shown to be related to the corresponding quantities at the left end through the relation of the form (Pestel and Leckie 1963)

$$\begin{Bmatrix} M(\omega) \\ \theta(\omega) \end{Bmatrix}_R = [T(\omega)] \begin{Bmatrix} M(\omega) \\ \theta(\omega) \end{Bmatrix}_L \tag{23}$$

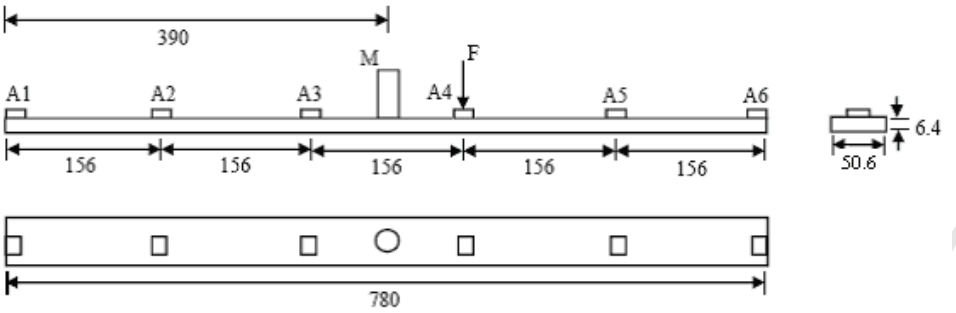

Figure 10: Free-free beam in undamaged state considered in example 5.2; A1-A6 indicate accelerometers; F indicates the force applied through impulse hammer; M is a concentrated mass; damaged structure is created by removal of mass M; all dimensions are in mm.

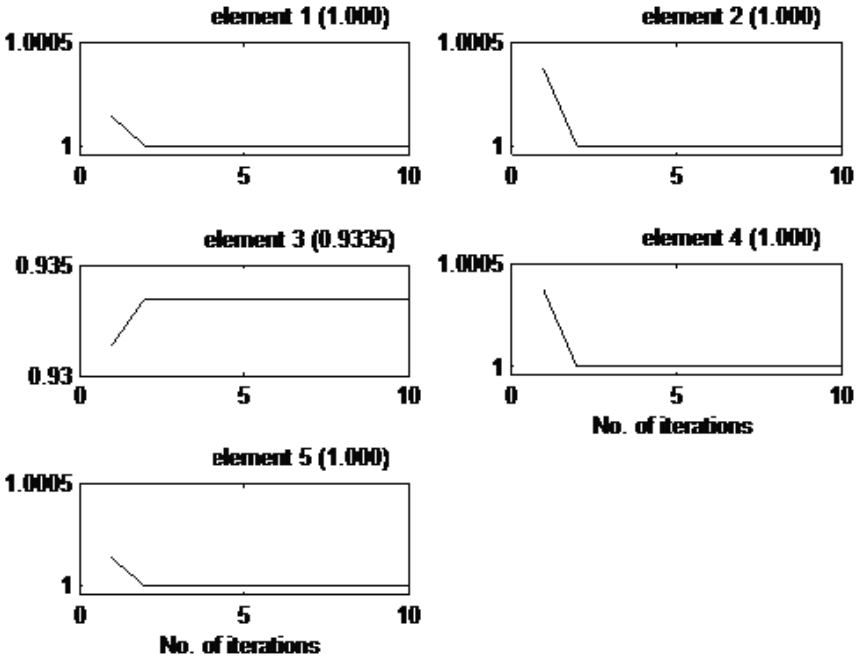

Figure 11: Example 5.2; results on damage detection using Method II; damage indication factors for mass; reference values are indicated in the parenthesis.

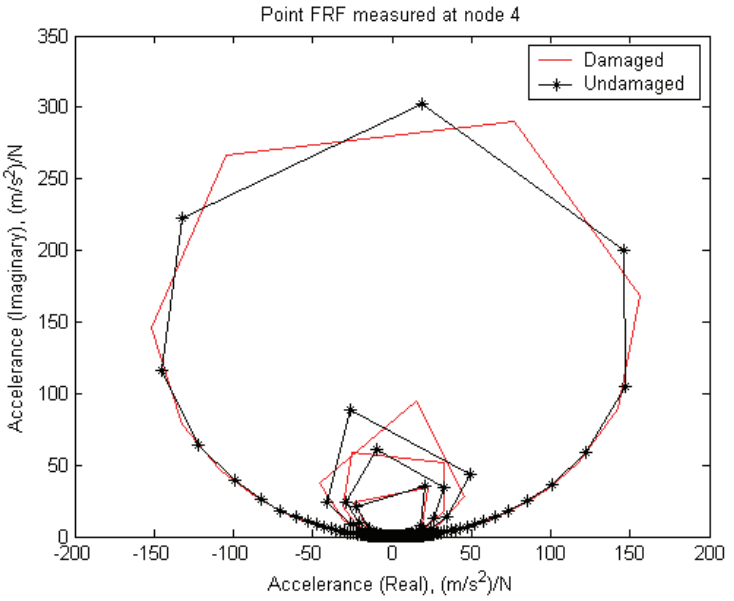

(a)

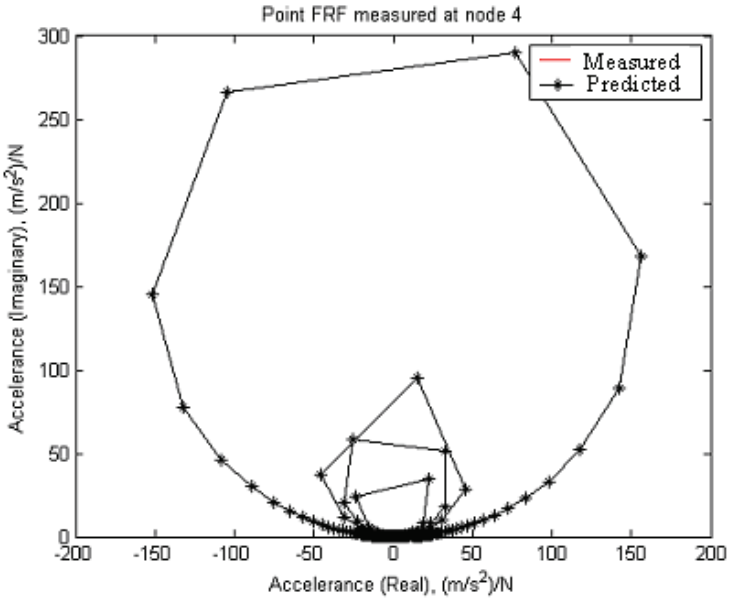

(b)

Figure 12: Example 5.2; results on damage detection using Method II; (a) System FRF in damaged and undamaged states; (b) comparison of measured and predicted FRF-s of the damaged system; note that the damage detection using Methods I and II are equally successful and the two results overlap.

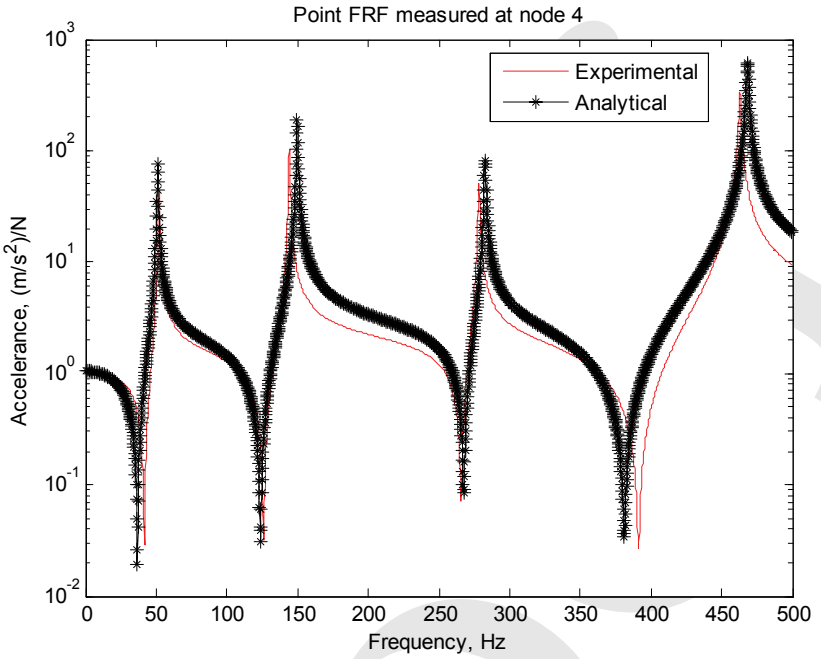

Figure 13: Example 5.2; results on damage detection using Method II.

Here T is the 2×2, frequency dependent, system transfer matrix. If one considers a periodic structure, with the beam unit in figure 14 as the repeating unit, clearly, the propagation of a traveling wave in such a system would be governed by the eigenvalues of the matrix T. These eigenvalues are known to occur in reciprocal pairs. By denoting the eigenvalues as $\lambda_{1,2}$ and, introducing the notation $\lambda_{1,2} = \exp[\pm(\gamma + i\kappa)]$, we observe that the nature of spatial variation of the waves depends on the attenuation constant γ. Clearly, for spatial periodic motions to be possible, it is required that $\gamma(\omega) = 0$ (here ω is said to belong to the 'pass' band) otherwise the waves would attenuate (here ω will be in the 'stop' band). For the purpose of illustration, we consider a four span continuous beam that is perfectly periodic (individual span=0.5m, E=2.0E+11 N/m^2, area of cross section= 98.84 mm^2, density=7483.2 kg/m^3). Figure 15 shows the spectrum of the attenuation constant which clearly depicts the occurrence of alternating sequence of stop and pass bands. Furthermore, the figure also shows the natural frequencies of the four span beam and these frequencies are seen to occur in clusters of four with each cluster lying within a pass band. To demonstrate the effect of modifying the structure which leads to the breaking of periodicity, we consider the density of the material in

the second span to be increased by 50%. The resulting changes in natural frequencies of the system are shown in figure 16 in which the spectrum of the attenuation constant of the perfectly periodic beam is also shown. It may be observed from the plot that some of the natural frequencies of the disordered beam now lie in the stop bands of the perfectly periodic beam. The mode shapes associated with these natural frequencies display spatial attenuation characteristics (figure 17) and the mode is said to be spatially localized. While this phenomenon has been the subject of extensive research in structural mechanics literature, it appears that the inverse problem associated with SSI and SDD as applied to this class of structures has not received wide attention.

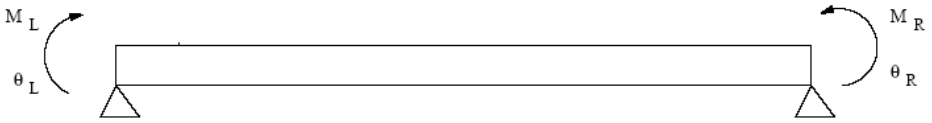

Figure 14: One span beam unit.

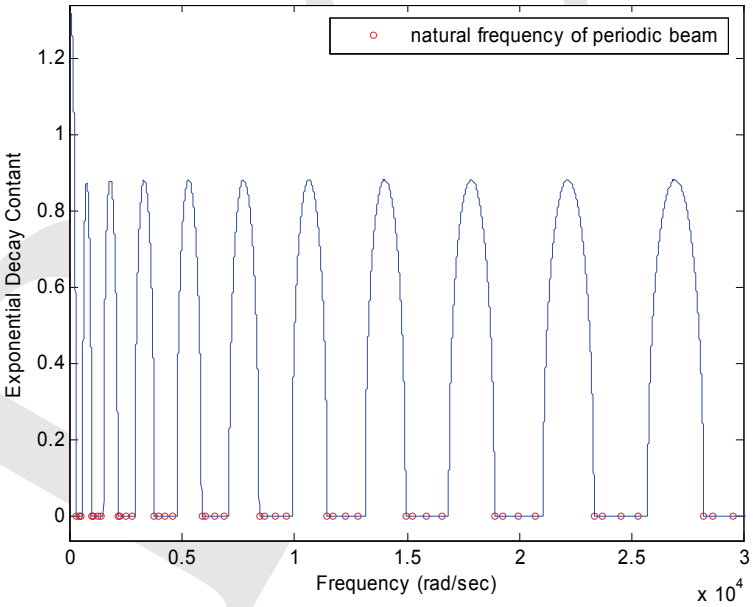

Figure 15: Spectrum of the attenuation constant for a perfectly periodic beam; the circles show the natural frequencies occurring in clumps within the pass bands.

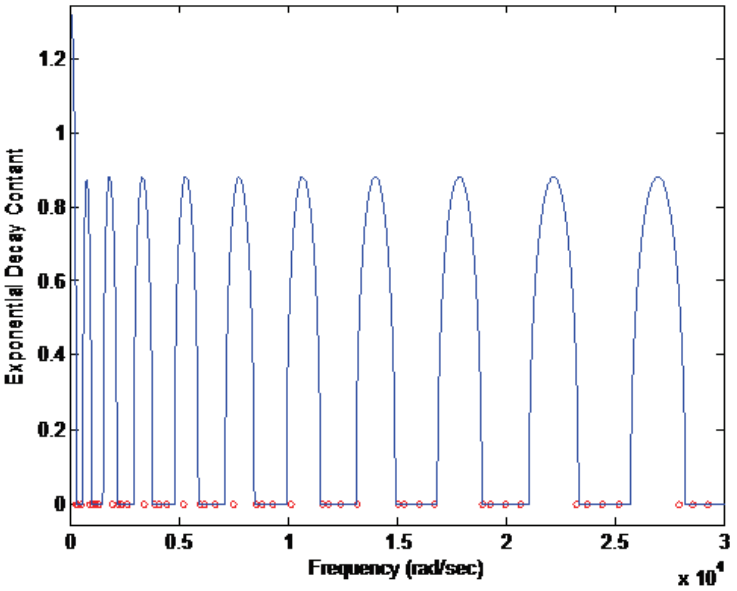

Figure 16: Spectrum of the attenuation constant for a perfectly periodic beam; the circles show the natural frequencies of the disordered beam.

Table 2: Properties of the four span steel beam considered in section 5.3

Total length	2.0 m
Length of each span	0.50 m
Width	24.9590 mm
Thickness	3.9620 mm
Mass density	7483.250 kg/m^3
Modulus of elasticity	2.0e11 N/m^2
Concentrated mass M	37.550 g
Added mass (m)	8.670 g
Mass A1-A7	8.670 g
Rayleigh's damping parameters	$\xi_{ms} = 10.7117$ & $\xi_{ks} = 1.9360E-06$
Rotational stiffness at each support (Nm/rad)	892.5, 811.5, 805.5, 830.5, 913.0

In the present study we consider the four span steel structure shown in figure 18. This model serves as the first cut physical model for an experimental model that the authors are currently studying. M denotes a point mass which can be either added

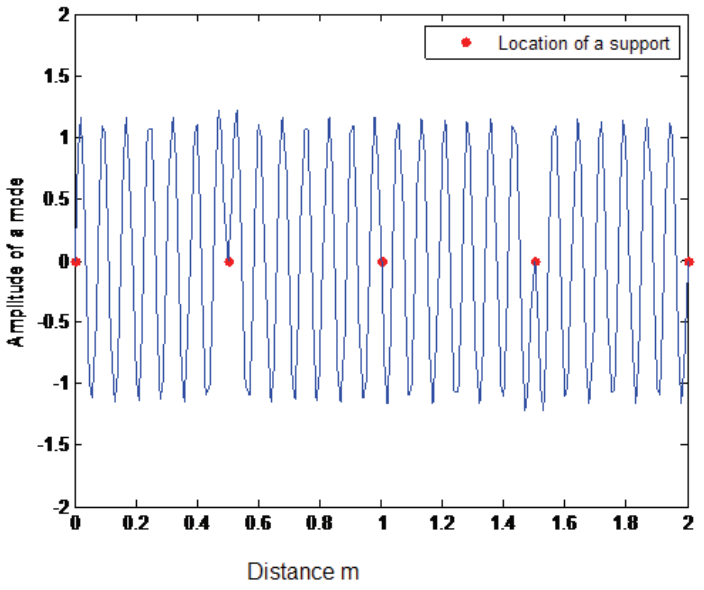

(a)

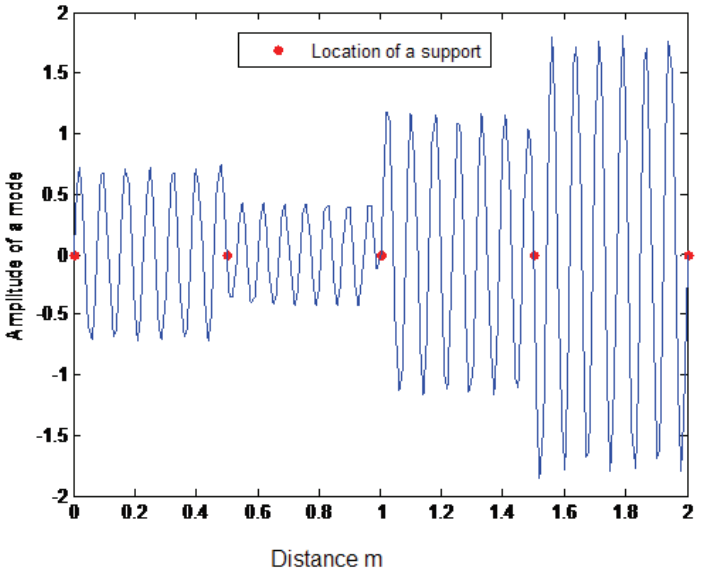

(b)

Figure 17: Normal modes of multi-span beam (a) Extended mode of perfectly periodic structure; (b) localized normal mode of disordered structure.

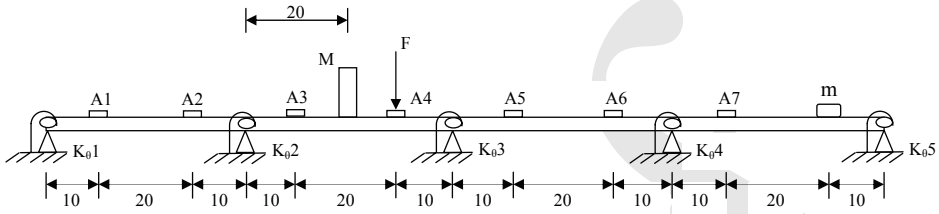

Figure 18: Example 5.3; M= a point mass that is introduced to create disorder; A1-A7: accelerometers; m=dummy mass introduced to retain periodicity of the structure; $K_{\theta i}; i = 1,2,\ldots,5$are the rotary springs to correct for imperfect simply supported end conditions; all dimensions are in mm.

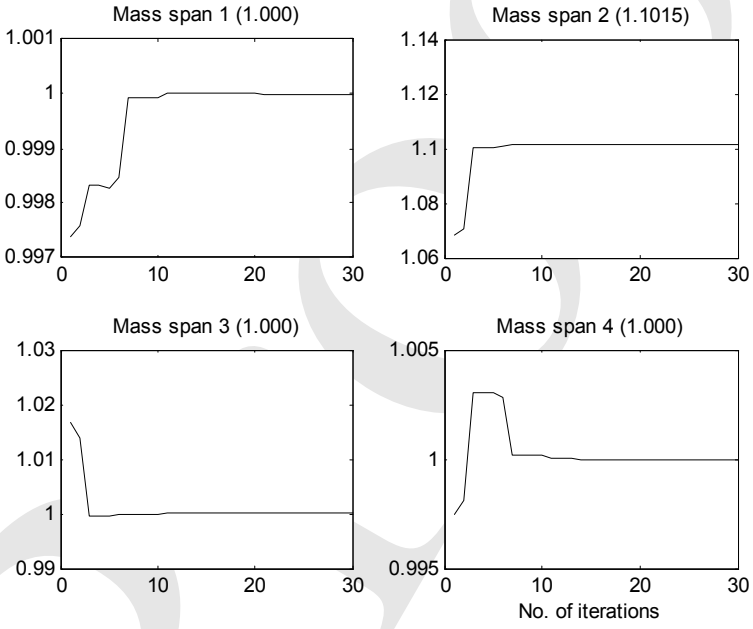

Figure 19: Example 5.3; detection of changes in mass parameters using inverse sensitivity of singular solutions; reference values are indicated in the parenthesis.

or removed to create disorder in the system; A1-A7 indicate the accelerometers and a point mass m is added in the fourth span to ensure that all the spans are identical; $K_{\theta i}$; $i = 1,2,\ldots,5$ denote tensional springs that are introduced to model imperfect simple support conditions in the experimental fixture. Table 2 summarizes the properties of the structure. In implementing the identification algorithm, the structure is

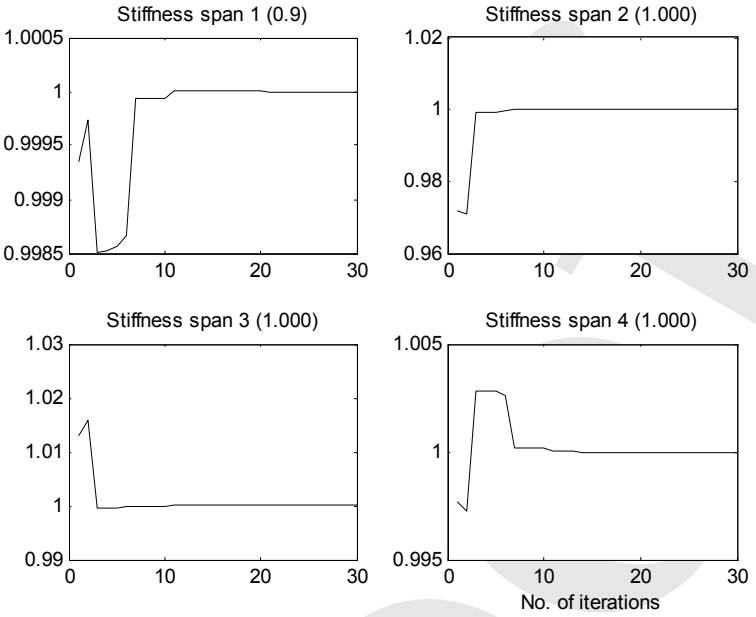

Figure 20: Example 5.3; detection of changes in stiffness parameters using inverse sensitivity of singular solutions; reference values are indicated in the parenthesis.

modeled using 80 number of 2-noded, Euler-Bernoulli beam elements with 2 dofs per node. The beam is further dived into four zones and properties within each zone are taken to be constant. The damping matrix within each of these zones is taken to be of the Rayleigh type with the matrix being a linear combination of the mass and stiffness matrices. The mass density, flexural rigidity and proportionality constants appearing in the damping model in each of the four zones are treated as parameters to be identified. Additionally, the torsional springs at the supports are also taken to be parameters to be identified. Thus, in this example we have 21 parameters to be identified. The structure in its undamaged state is given by the system with M=0 and the in the 'damaged' structure the mass M=37.55 g is introduced. We employ the method based on inverse sensitivity of singular value and the left singular vector of a 7×1FRF matrix to detect the changes in the 21 parameters of the system. This FRF matrix is obtained by driving at A4 and measuring response accelerations at the points A1-A7 (figure 18). Figures 19 and 21 show a selection of results and these figures illustrate identification of mass and stiffness parameters. The drive point accelerances of the system in its damaged and damaged states are superposed in figure 21. The successful performance of the SDD can be evidenced in figure 22 in which the predicted drive point accelerance of the damaged system is observed

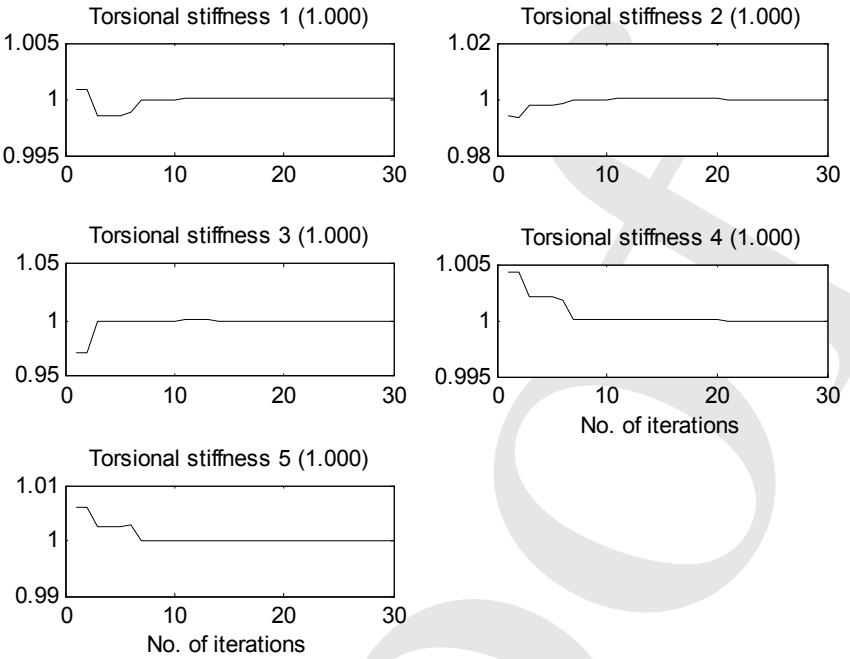

Figure 21: Example 5.3; detection of changes in support stiffness parameters using inverse sensitivity of singular solutions; reference values are indicated in the parenthesis.

to match very well with the measured accelerance.

5 Closing remarks

The problem of structural damage detection, location and quantification in linear time invariant structural dynamical systems has been considered in this study by using singular solutions of the system FRF matrix as response features for damage characterization. The study assumes that a baseline mathematical model of the structure in its undamaged state is available. The proposed method is capable of detecting changes to mass, stiffness and (or) damping characteristics of the system. For systems with well separated modes, the proposed method conceptually encompasses in its fold the inverse sensitivity methods based on eigensolutions and FRF-s. Thus we note the following:

By selecting the frequencies of interest to coincide with the system natural frequencies, and by taking the first singular solution as the response feature of interest, the present method becomes nearly the same as the method that uses inverse sensitivity

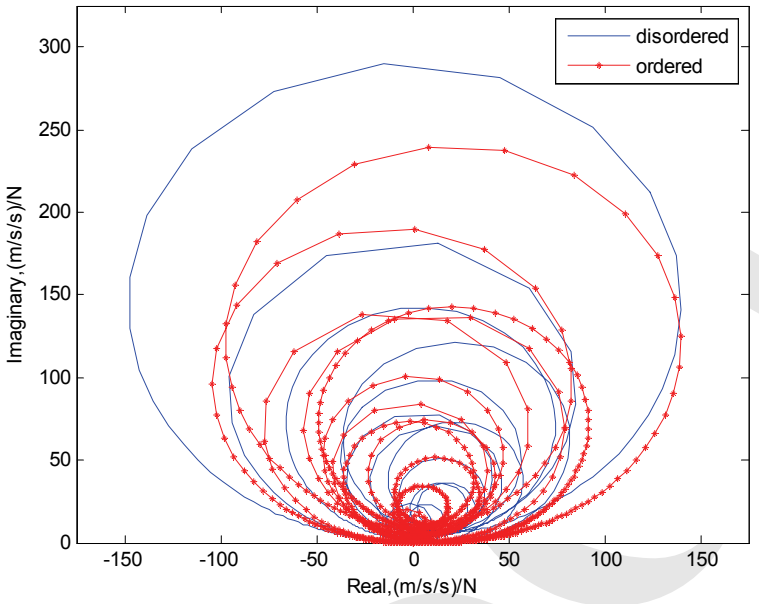

Figure 22: Example 5.3; Nyquist plot of the drive point accelerance for the structure in its damaged and undamaged states.

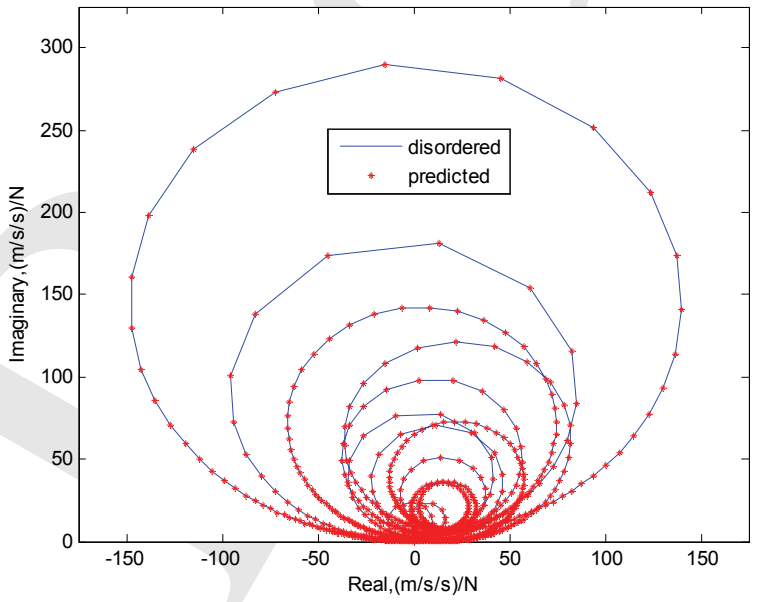

Figure 23: Example 5.3; Nyquist plot of the drive point accelerance for the structure in its damaged state and the prediction of the accelerance after damage detection.

of natural frequencies alone.

In addition to the first singular value as in the item above, if we also include the first left singular vector as an additional response feature, the procedure becomes nearly the same as the method that uses inverse sensitivity of natural frequencies and mode shapes.

If we include all the singular values and singular vectors at all the frequencies, the method is equivalent to inverse sensitivity method based on FRF-s.

Thus, the method has the inherent ability to selectively include key features of system response and permits an increasingly elaborate analysis of measured data with a view towards structural damage characterization. More importantly, the method is particularly suited for damage detection in systems with repeated or closely spaced modes. This has been exemplified in the present study by considering damages to system with repeated natural frequencies and also spatially periodic structures in which the natural frequencies occur in packets of closely spaced modes.

References

Aktan A. E., Farhey D. N., Helmicki A. J., Brown D. L., Hunt V. J., Lee K. L., Levi A. (1997): Structural identification for condition assessment: Experimental arts, *Journal of Structural Engineering, ASCE*, 123(12), 1674-1684.

Alvandi A., Cremona C. (2005): Assessment of vibration-based damage identification techniques, *Journal of Sound and Vibration*, 292(1-2), 179-202.

Allemang R. J., Brown D. L. (1998): A unified matrix polynomial approach to modal identification, *Journal of Sound and Vibration*, 211(3), 301-322.

Bendat J. S., Piersol A. G. (1980): *Engineering application of correlation and spectral analysis*, John Wiley and Sons, New York.

Brillouin, L. (1958): *Wave propagation in periodic structures*, Dover, New York.

Cawley P., Adams R. D. (1979): The location of defects in structures from measurements of natural frequencies, *Journal of Strain Analysis*, 14(2), 49-57.

Cha P. D., Switkes P. (2002): Enforcing structural connectivity to update damped systems using frequency response, *AIAA Journal*, 40(6), 1197-1203.

Doebling S. W., Farrar C. R., Prime M. B. (1998): A summary Review of vibration-based damage identification methods, *Shock and Vibration Digest*, 30(2), 91-105.

Ewins D. J. (2000): *Modal testing: Theory, Practice and Application*, Research studies press limited, Baldock, Hertfordshire.

Farhat C., Hemez F. M. (1993): Updating finite element dynamic models using

an element-by-element sensitivity methodology, *AIAA Journal*, 31(9), 1702-1711.

Friswell M. I., Mottershead J. E. (1996): *Finite element model updating in structural dynamics*, Kluwer Academic Publishers, Dordrecht.

Forth S. C., Staroselsky, A. (2005): A Hybrid FEM/BEM Approach for Designing an Aircraft Engine Structural Health Monitoring, *CMES: Computer Modeling in Engineering and Sciences*, 9(3), 287-298.

Ge M., Lui E. M. (2005): Structural damage identification using system dynamic properties, *Computers and Structures*, 83, 2185-2196.

Hansen P. C. (1994): Regularization tools: A Matlab package for analysis and solution of discrete ill-posed problems, *Numerical Algorithms*, 6, 1–35.

Hearn G., Testa R. B. (1991): Modal analysis for damage detection in structures, *Journal of Structural Engineering, ASCE*, 117(10), 3042-3063.

Hodges, C. H. (1982): Confinement of vibration by structural irregularity, *Journal of Sound and Vibration*, 82, 411-424.

Hsieh K. H., Halling M. W., Barr P. J. (2006): Overview of vibrational structural health monitoring with representative case studies, *Journal of Bridge Engineering, ASCE*, 11(6), 707-715.

Huang C. H., Shih, C. C. (2007): An inverse problem in estimating simultaneously the time dependent applied force and moment of an Euler-Bernoulli beam, *CMES: Computer Modeling in Engineering and Sciences*, 21(3), 239-254, 2007.

Huynh D., He J., Tran D. (2005): Damage location vector: A non-destructive structural damage detection technique, *Computers and Structures*, 83, 2353-2367.

Law S. S., Shi Z. Y., Zhang L. M. (1998): Structural damage detection from incomplete and noisy modal test data, *Journal of Engineering Mechanics, ASCE*, 124(11), 1280-1288.

Lee I. W., Jung G. H. 1997a, An efficient algebraic method for the computation of natural frequency and mode shape sensitivities- part I: Distinct natural frequencies, *Computers and Structures*, 62(3), 429-435.

Lee I. W., Jung G. H. 1997b, An efficient algebraic method for the computation of natural frequency and mode shape sensitivities- part II: Multiple natural frequencies, *Computers and Structures*, 62(3), 437-443.

Lee J. H., Kim J. (2001): Identification of damping matrices from measured frequency response functions, *Journal of Sound and Vibration*, 240(3), 545-565.

Lin R. M., Lim M. K., Du H. (1995): Improved inverse eigensensitivity method for structural analytical model updating, *Transactions of the ASME, Journal of Vibration and Acoustics*, 117, 192-198.

Liu, C. S. (2008): A Lie-Group Shooting Method for Simultaneously Estimating the Time-Dependent Damping and Stiffness Coefficients, *CMES: Computer Modeling in Engineering and Sciences*, 27(3), 137-150.

Manohar C. S., Ibrahim, R. A. (1999): Progress in structural dynamics with stochastic parameter variations 1987-1998, *Applied Mechanics Reviews*, 52(5), 177-197.

Maia N. M. M., Silva J. M. M. (1997): *Theoretical and experimental modal analysis*, Research Studies Press Limited, Taunton, Somerset, England.

Maia N. M. M., Silva J. M. M., Almas E. A. M. (2003): Damage detection in structures: From mode shape to frequency response function methods, *Mechanical Systems and Signal Processing*, 17(3), 489-498.

McConnel (1995): *Vibration testing: Theory and practice*, John Wiley, New York.

Mead D. J. (1996): Wave propagation in continuous periodic structures: research contributions from Southampton, 1964-1995, *Journal of Sound and Vibration*, 190(3), 495-524.

Meirovich L. (1984): *Elements of vibration analysis*, McGraw Hill, New York

Necati C. F., Brown, D. L., Aktan, E. (2004): Parameter estimation for multiple-input multiple-output modal analysis of large structures, *Journal of Engineering Mechanics, ASCE*, 130(8), 921-930.

Nobari A. S. (1991): *Identification of the dynamic characteristics of structural joints*, PhD thesis, Imperial College of Science, Technology and Medicine, University of London.

Park N. G. Park Y. S. (2003): Damage detection using spatially incomplete frequency response functions, *Mechanical Systems and Signal Processing*, 17(3), 519-532.

Peeters B., Roeck G. D. (2001): Stochastic system identification for operational modal analysis: A review, *Transactions of the ASME, Journal of Dynamic Systems, Measurement and Control*, 123, 659-667.

Pestel E. C., Leckie, F. A. (1963): *Matrix methods in elastomechanics*, McGraw-Hill, New York.

Petyt M. (1998): *Introduction to finite element vibration analysis*, Cambridge University Press.

Ratcliffe C. P. (2000): A frequency and curvature based experimental method for locating damage in structures, *Transactions of the ASME, Journal of Vibration and Acoustics*, 122, 324-329.

Reddy K. V., Ganguli, R. (2007): Fourier analysis of mode shapes of damaged

beams, *CMC: Computers, Materials and Continua*, 5(2), 79-98.

Salawu S. (1997): Detection of structural damage through changes in frequency: A review, *Engineering Structures*, 19(9), 718-723.

Sanayei M., McClain A. S., Fascetti S. W., Santini E. M. (1999): Parameter estimation incorporating modal data and boundary conditions, *Journal of Structural Engineering, ASCE*, 125(9), 1048-1055.

Sengupta G. (1980): Vibration of periodic structures, *The Shock and Vibration Digest*, 12(3), 17-29.

Shih C. Y., Tsuei Y. G., Allemang R. J., Brown D. L. (1988): Complex mode indication function and its applications to spatial domain parameter estimation, *Mechanical Systems and Signal Processing*, 2(4), 367-377.

Sohn H., Farrar C. R., Hemez F. M., Czarnecki J. J., Shunk D. D., Stinemates D. W., Nadler B. R. (2003): A review of structural health monitoring literature: 1996-2001, *Los Alamos National Laboratory Report*, LA-13976-MS.

Strang G. (1980): *Linear Algebra and its Applications*, Academic Press, New York.

Tabrez S., Mitra M., Gopalakrishnan S. (2007): Modeling of degraded composite beam due to moisture absorption for wave based detection, *CMES: Computer Modeling in Engineering and Sciences*, 22(1), 77-90.

Venkatesha S. (2007): *Inverse sensitivity methods in linear structural damage detection using vibration data*, MSc (Engg.) Thesis, Department of Civil Engineering, Indian Institute of Science, Bangalore, India.

Visser W. Y. (1992): *Updating structural dynamic models using frequency response data*, PhD thesis, Imperial College of Science, Technology and Medicine, University of London.

Wang Z., Lin R. M., Lim M. K. (1997): Structural damage detection using measured FRF data, *Computer Methods in Applied Mechanics and Engineering*, 147, 187-197.

Wang, K., Zhou S., Nie Z., Kong S. (2008): Natural neighbor Petrov-Galerkin Method for Shape Design Sensitivity Analysis, *CMES: Computer Modeling in Engineering and Sciences*, 26(2), 107-122.

Appendix A

Here we consider a 7-dof system with the 7×7 mass and stiffness matrices given respectively by $M_{ii} = 100$ kg, $i = 1,2,\cdots,7$; $M_{ij} = 0\ \forall i \neq j$; $i, j = 1,2,\cdots,7$ and $K_{ii} = 7000\,\mathrm{N/m}$; $i = 1,2,\cdots,7$; $K_{ij} = -10000\,\mathrm{N/m}\ \forall i \neq j$; $i, j = 1,2,\cdots,7$. The undamped natural frequencies for the system are obtained as ω_1=10 rad/s and

$\omega_2 = \omega_3 = \cdots = \omega_7$= 28.28 rad/s. Figure A.1 shows a few of the system FRF-s obtained under the assumption that the system is viscously damped with damping ratio in all the modes being equal to 0.02. Given that one of the natural frequencies of the system is already known to repeat six times, as one might expect the FRF-s show only two peaks although the system itself has 7 dofs. This deduction, however, would not be straightforward if the FRF-s are obtained experimentally and they could as well be mistaken for response of a 2-dof system. The singular solutions of the FRF matrix serve useful purpose in this context in determining the number of modes present in a measured FRF. Figure A.2 show the spectrum of the singular solutions (based on the 7×7FRF matrix). The first singular solution shows two peaks and the second peak repeats prominently in the next five singular value spectra. This leads to the conclusion that the FRF-s are originating from a system with seven dofs. If we change the mass matrix such that $M_{11} = 100, M_{22} = 2004, M_{33} = 300, M_{44} = 250, M_{55} = 400, M_{66} = 50, M_{77} = 90\,\text{kg}$; $M_{ij} = 0\ \forall i \neq j$; $i, j = 1, 2, \cdots, 7$ and keep the stiffness matrix as above, the system would now possess 7 distinct natural frequencies (6.92, 15.00,17.13, 19.23, 25.77, 29.18, and 28.26 rad/s). A few of the FRF-s for the system are shown in figure A.3 and the spectrum of singular values here are as shown in figure A.3. These spectra corroborate the fact that the system has 7 distinct natural frequencies.

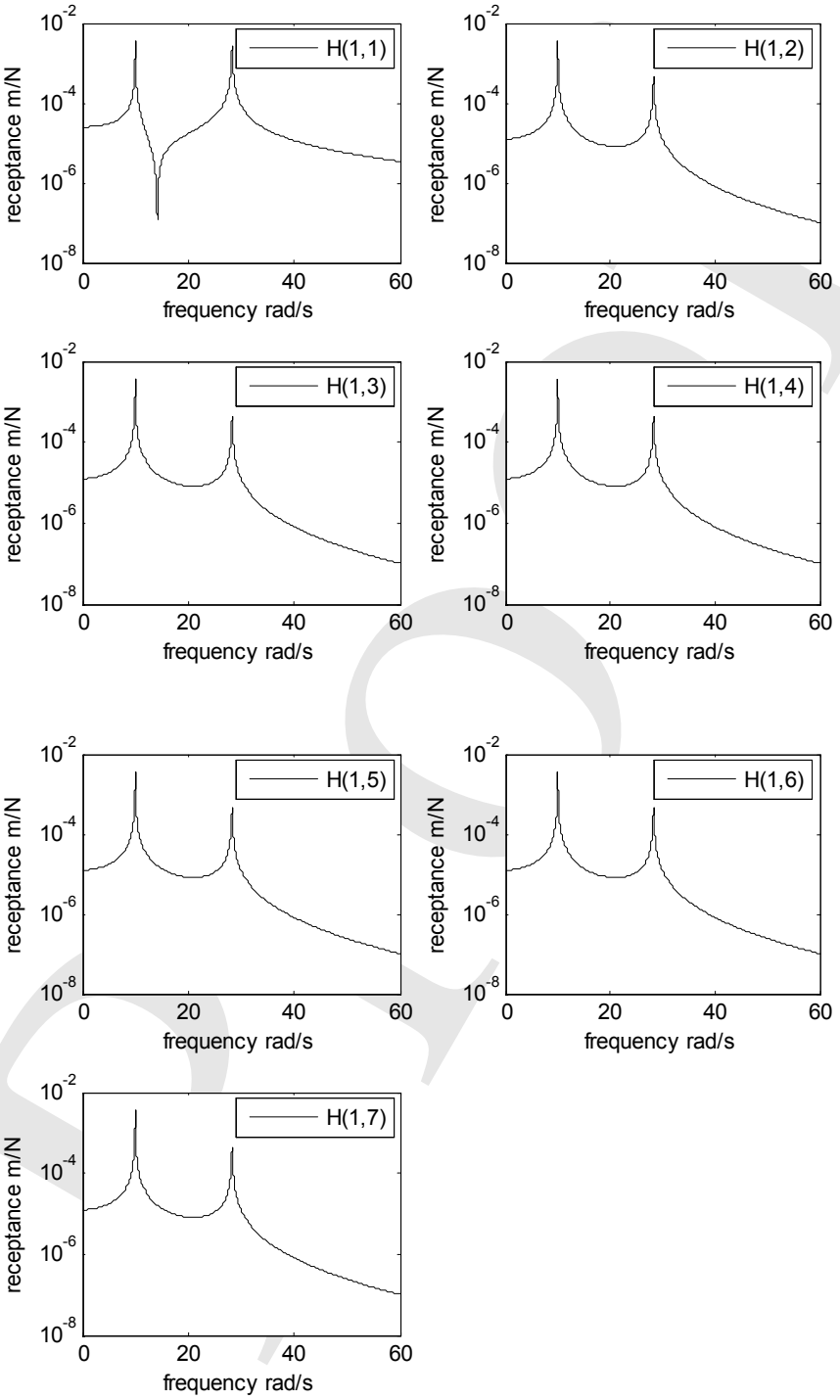

Figure A.1: Receptance functions for the 7-dof system considered in Appendix A; system with repeated natural frequencies.

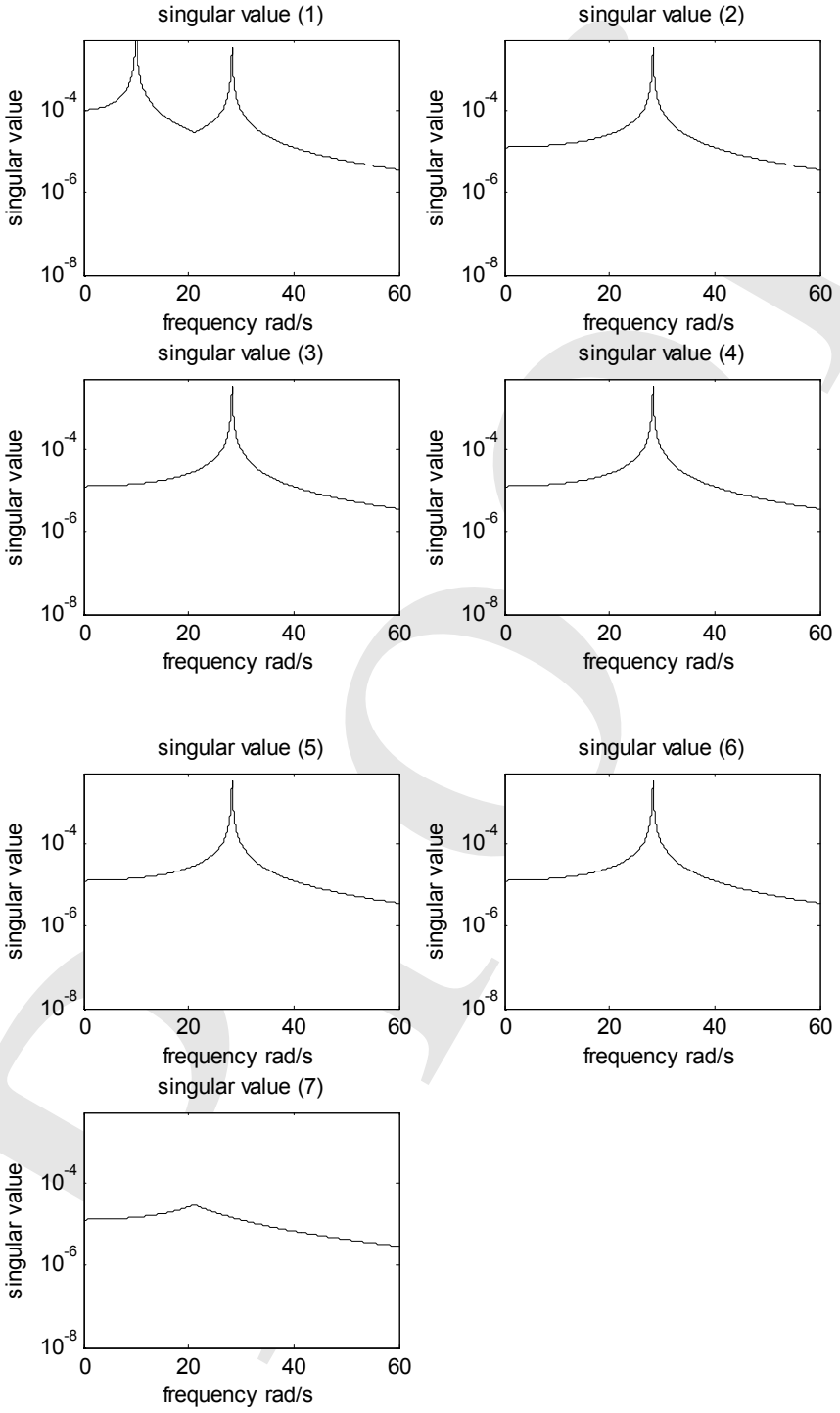

Figure A.2: Singular values of FRF matrix considered in Appendix A; system with repeated natural frequencies.

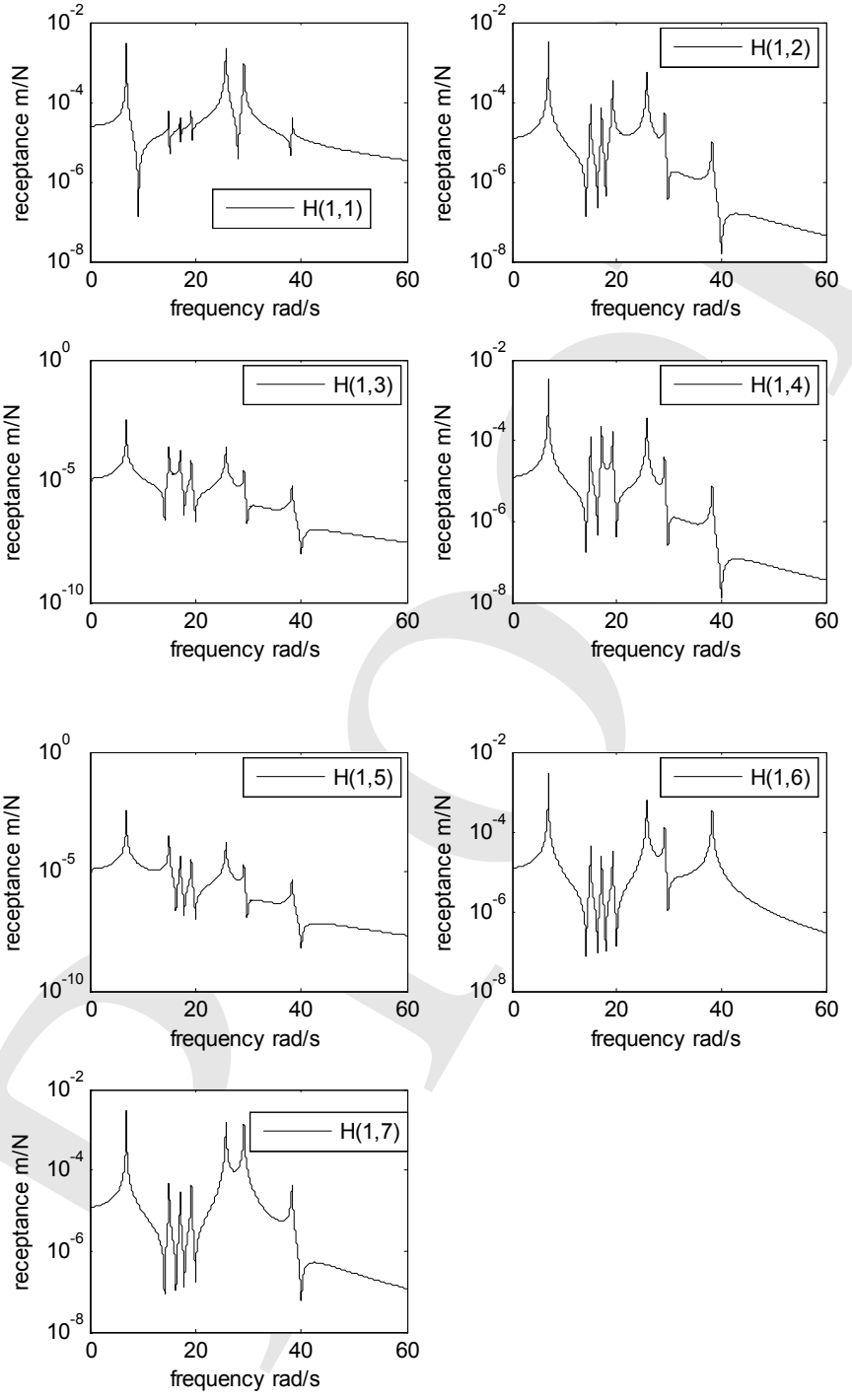

Figure A.3: Receptance functions for the 7-dof system considered in Appendix A; system with distinct natural frequencies.

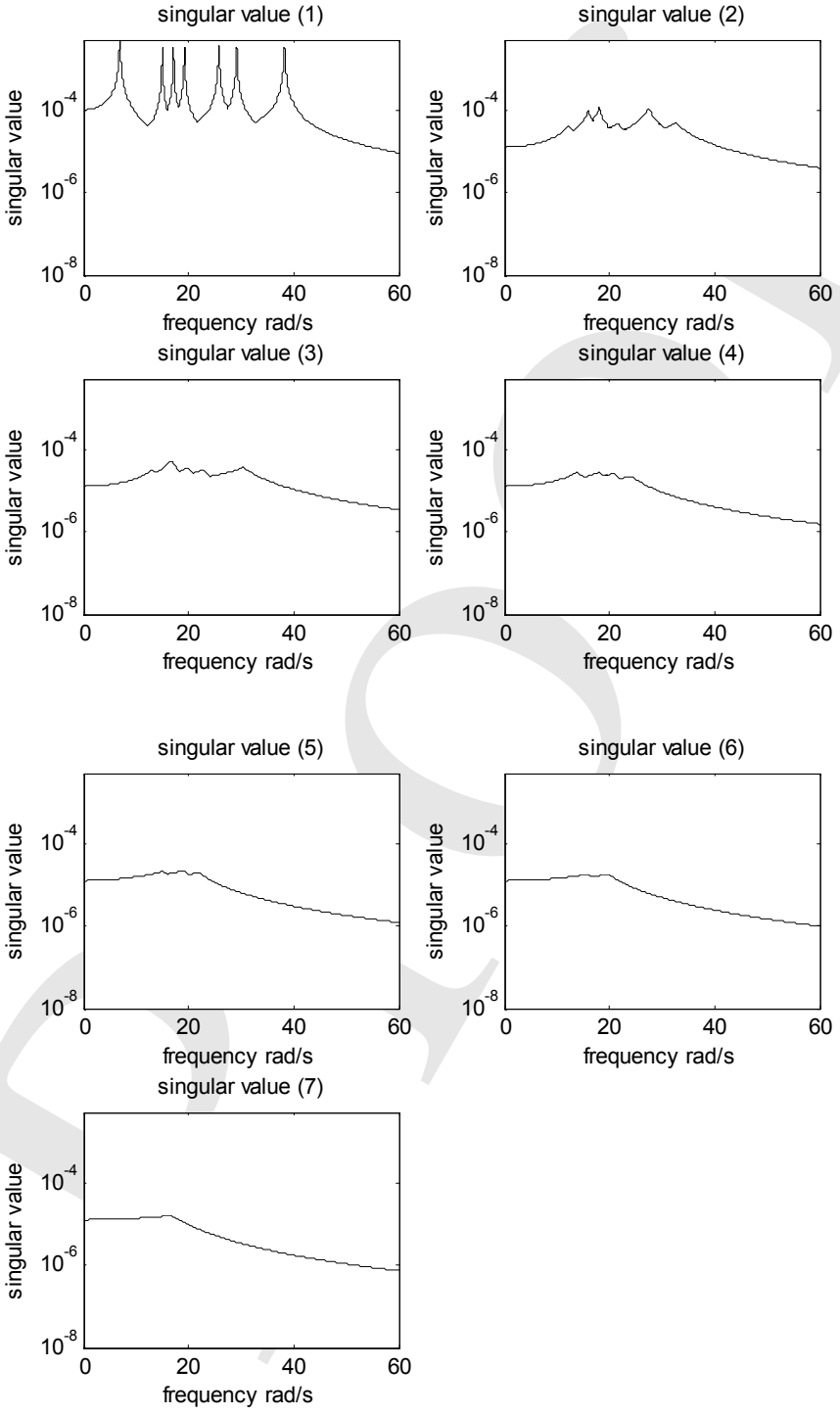

Figure A.4: Figure A.4 Singular values of FRF matrix considered in Appendix A; system with distinct natural frequencies.